PHYSICAL REVIEW A **72**, 032714 (2005)

Distorted-wave theory for positron-hydrogen collisions

Arijit Ghoshal[1] and Puspajit Mandal[2]
[1]*Department of Mathematics, Suri Vidyasagar College, Suri 731 101 West Bengal, India*
[2]*Department of Mathematics, Visva-Bharati University, Santiniketan 731 235 West Bengal, India*

(Received 25 March 2005; published 14 September 2005)

The scattering amplitude for positron-hydrogen collisions has been conveniently derived within the framework of distorted-wave theory by approximating the distortion potential in a particular channel as the average of perturbation of that particular channel over the bound states. A real advantage of this method is that a few straightforward calculations yield the expression of scattering amplitude as a function of partial wave. The method has been successfully applied to study $1s$-$2s$ excitation of hydrogen atom by positron impact and Ps (ns) $(n=1,2,3)$ formation in positron-hydrogen collisions in the intermediate and high energy range. Further to bring the scattering amplitudes in tracktable forms we have formulated an effective and efficient method for evaluating general three-denominator Lewis integral. The results compare nicely with other theoretical and experimental results available in the literature.

DOI: 10.1103/PhysRevA.72.032714 PACS number(s): 34.85.+x, 36.10.−k, 03.65.Nk

I. INTRODUCTION

Most of the theoretical calculations pertaining to the quantum collisions theory can be broadly classified into two categories, namely, nonperturbative calculations and perturbative calculations. Variational methods and close-coupling approximations that are being widely used in atomic collisions problems are of nonperturbative nature. The ability of such methods of obtaining definitive results of quantum collision phenomena in low and intermediate energy range has been firmly established over the years. On the other hand, since the early days of quantum mechanics, attempts have been made to suitably approximate the series resulting from the iterative solution of the Lippmann-Schwinger integral equation so that satisfactory results could conveniently be obtained. In such a process of approximation, either the wave function or the actual potential or both are perturbed considering the features of the system concerned in order to obtain expressions that can be conveniently evaluated. Born series, distorted-wave series, the eikonal Born series fall under such perturbative calculations.

It is well known that the Born series converges too slowly for direct collisions and is useful in practical calculations in the high energy range. As a matter of fact all theoretical calculations converge in Born series at very high energies. Distorted-wave series, on the other hand, which replace plane waves in the matrix of collision amplitude converges more rapidly and has the efficiency for predicting reliable results in intermediate and high energy region. This efficiency, of course, rests on the fitness of distortion made upon the wave function or the potential of the concerned system.

Over the past few years, the distorted-wave approximation (DWA) has been widely applied to calculate scattering cross sections for electron-atom collisions [1–18], electron-molecule collisions [19–22] and positron-atom collisions [25–30]. The first calculations with this approximation were carried out by Erskine and Massey [1]. They calculated the distorted-wave functions by the Kohn variational method to compute $1s$-$2s$ excitation of hydrogen atom by electron impact. Inclusion of distortion had the drastic effect of reversing the relative importance of the symmetric and antisymmetric cross sections as compared with the Born-Oppenheimer approximation. Ochkur [2] repeated these calculations using distorted-waves obtained by accurate numerical solution, with electronic computation, of the integro-differential equations involved. His results differ substantially from those of Erskine and Massey [1], particularly at energies close to the thresholds.

Calculations using distorted-wave approximation, with full allowance for exchange, have been carried out by Massey and Moiseiwitch for the excitation of the $2\,^1S, 2\,^3S$ [3], and $2\,^3P$ [4] states from the ground state of helium atom by electron impact. Superelastic collisions, in which $2\,^1S$ metastable atoms are deactivated to the $2\,^3S$ state, have been more extensively studied by Marriott [5] using distorted-wave theory. Levenson and Banerjee [23] also carried out a detailed calculation using the full optical distorted-wave formula to calculate the angular distributions of nucleons inelastically scattered in reaction $C^{12}(p,p')C^{12*}$ from ground state (O^+) to the first excited state (2^+)) at sufficiently high energies. Later Khashaba and Massey [6] used distorted-wave theory to calculate $1s$-$2p$ excitation cross section of hydrogen by electron impact.

The first rigorous formulation of the distorted-wave theory for rearrangement collisions was made by Bassel and Gerjuoy [24]. Removing the unphysical internuclear Coulomb interaction from the perturbation Hamiltonian they were able to obtain an elegant expression for arbitrary rearrangement collisions. Applying the procedure to the problem of electron capture by protons in atomic hydrogen in the high energies they obtained results that are in good agreement with experiment.

In another development Madison and Shelton [8] applied the distorted-wave theory for electron-impact excitation of $6s6p\,^1P_1$ state of mercury and obtained results for polarization and differential cross section in accord with the experimental data. They [8] also used this distorted-wave theory to calculate the excitation cross section of helium from its ground state to the $1s2p\ {}^1P_1$ excited state for incident electron energies between 26.5–300 eV. Madison [13] and Madison *et al.* [14] further carried forward this work. The authors reported a second-order distorted-wave calculation (DWB2) to explicitly sum over all contributing bound states and integrate over all contributing continuum intermediate states. Calculations were then performed for excitation of the $2p$ [15] and $2s$ [16] states of hydrogen and the exact results were used to examine the validity of the closure approximation and the pseudostate approximation.

In case of positron-hydrogen system, Mandal, Guha, and Sil [25] applied an all-order distorted-wave theory to calculate the ground-state positronium formation. Mandal and Guha [26] further studied the same system using a first-order distorted-wave theory. The integrated cross sections obtained by using these two approximations agree nicely at intermediate and high energies.

Later Shakeshaft and Wadehra [27], with distortion included through first order, elaborately studied ground-state-to-ground-state electron capture by positrons from hydrogen atom. Their computed cross sections are close to those of Mandal, Guha, and Sil [25], and Mandal and Guha [26]. Subsequently Khan and Ghosh [28] also evaluated the cross section for the ground-state Ps formation in positron-hydrogen collisions within the framework of distorted-wave theory in which total incident wave function was determined by the polarized orbital methods. Afterward Srivastava *et al.* [29] investigated positron-hydrogen system employing a first-order distorted-wave method which takes into account long-range effects through the use of a polarization potential.

In a further development of the distorted-wave theory, Madison, Bray, and McCarthy [17] elaborately demonstrated the feasibility of the distorted-wave calculations exact to the second order. Taking into account the second-order exchange they were able to predict reliable results for elastic electron-hydrogen scattering above 30 eV and $2s$, $2p$ excitation of hydrogen atom by electron impact above 50 eV. Later, using this formulation for positron-hydrogen system, Bubelev and Madison [30] reported results for elastic and inelastic scattering in the intermediate energy range. Their reported results were in close agreement with the other available theoretical calculations.

To gain a deeper understanding of the validity of DWA, Lee *et al.* [21] made a comparative study of the distorted-wave approximation for electron-H_2 collisions with the two-channel Schwinger method. The authors observed a general good agreement for the excitation cross section of $b\ {}^3\Sigma_a^+, a\ {}^3\Sigma_g^+$, and $c\ {}^3\Pi_a$ between both theories for the incident energies above 20 eV.

In a recent study, Colgan *et al.* [31] carried out distorted-wave calculations for the electron-impact ionization of atomic ions in the Mn isonuclear sequence. Of late, Zhangjin *et al.* [18] analyzed the triple differential cross sections for ionization of atomic hydrogen by electron impact in the case of coplanar, asymmetric geometry within the framework of second-order theory. They found that the second-order calculations represented a marked improvement over the results obtained from the first-order theories for higher impact energies above 150 eV.

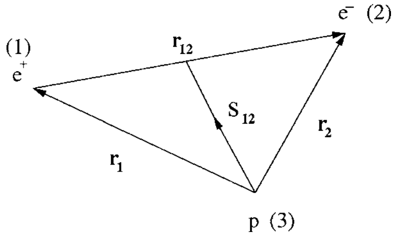

FIG. 1. Coordinate representation of positron-hydrogen system.

The objective of the present study is to formulate a viable scheme within the framework of the distorted wave theory that may be equally applicable to direct and rearrangement collisions processes at intermediate and high energies. As simple applications we study positron impact excitation of atomic hydrogen and positronium formation in hydrogen.

In Sec. II we develop the underlying theory and in Sec. III we apply this theory to the following processes:

(i) $1s$-$2s$ excitation of atomic hydrogen by positron impact,

(ii) Ps(ns) ($n=1,2,3$) formation in positron-hydrogen collisions.

The concluding remarks are made in Sec. IV and finally in the Appendixes we present an effective and efficient method for evaluating a general three-denominator Lewis integral to bring the scattering amplitudes in a tractable form.

II. THEORY

We denote the incident positron as particle 1, the bound electron as particle 2, and the proton as particle 3, considered to be infinitely heavy at the center of the coordinate system (Fig. 1). Neglecting a very small correlation (of the order electron mass and/or proton mass), the positron-proton interaction only depends on the coordinate r_1 and as such cannot induce a transition in the internal state of the target atom. The basic interaction responsible for such a transition in the internal state of the atom is the positron-electron correlation. In other words, if the positron-electron interaction is turned off, the internal state of the atom will remain the same. The only effect of the positron-proton interaction is to deflect the incident positron. Since the mass of the proton is very large compared to that of the positron and electron (1836:1), this deflection is of appreciable measure for low incident positron energy and consequently indirectly influences the internal structure of the atom. But with the increase in the incident positron energy this effect gradually slows down and hardly affects the probability of transition of the internal state of the atom in the intermediate and high energies. For electron capture at high energies, Shakeshaft *et al.* [27] has shown that the first and second order Born terms involving positron-proton interaction very nearly cancel. For heavy projectile at high energies it can be rigorously [37,38] proved that the electron capture cross sections is independent of projectile-proton interaction. It now appears legitimate to neglect the positron-proton interaction at intermediate and high energies to make our study more convenient. This is achieved by the so-called distorted-wave method which provides convenient means of removing the internuclear Coulomb interaction from the perturbation whose matrix element yields the cross sections. As a matter of fact the positron-proton interaction as well as all its dependence can conveniently be removed using the distortion potential as proposed by Bassel and Gerjuoy [24]. They chose the distortion potential in the initial channel as the average of actual perturbation of the initial channel with respect to the initial bound states and the distortion potential in the final channel as the average of actual perturbation of the final channel with respect to the final bound states. In other words, the distortion potential in the initial and final channels are the average (over internal motions) static interactions between the initial aggregates and final aggregates, respectively. With such a choice of the distortion potential, it can be shown that any term, in the actual potential, depending on r_1 only will not appear in the effective perturbations, the difference of actual and distortion potentials.

If H denotes the full Hamiltonian of the scattering system, it can be expressed in terms of the channel Hamiltonians as

$$H = H_i + V_i = H_f + V_f$$

such that

$$H_i\Phi_i = E_i\Phi_i, \quad H_f\Phi_f = E_f\Phi_f,$$

where Φ_i, Φ_f are the plane-wave states belonging to the Hamiltonians H_i and H_f in the incident and final channel, respectively, with residual interactions V_i and V_f having energies E_i and E_f,

$$E_\alpha = \frac{\hbar^2}{2\mu_\alpha}k_\alpha^2 + \epsilon_\alpha \quad (\alpha = i, f).$$

Here $(\epsilon_i, \epsilon_f), (\hbar k_i, \hbar k_f)$ are, respectively, the eigenenergies of bound states and positron momenta in the (incident, final) channels, whereas (μ_i, μ_f) are the reduced masses for the center of mass motion in the scattering system.

The energy conservation requires that, on the energy shell, $E_i = E_f = E$, the total energy of the system. The Green's operators are defined as

$$G_i^{\pm} = \frac{1}{E - H_i \pm i\epsilon}, \quad G_f^{\pm} = \frac{1}{E - H_f \pm i\epsilon}, \quad G^{\pm} = \frac{1}{E - H \pm i\epsilon},$$

the full scattering wave functions, $|\Psi_i^+\rangle, \langle\Psi_f^-|$ for the incident and final channels satisfy the Lippmann-Schwinger integral equations,

$$|\Psi_i^+\rangle = |\Phi_i\rangle + G_i^+ V_i |\Psi_i^+\rangle$$

and

$$\langle\Psi_f^-| = \langle\Phi_f| + \langle\Psi_f^-|G_f^- V_f.$$

The post and prior forms of the transition matrix from bound state i in the initial channel to the state f in the final channel may now be defined, on the energy shell, as

$$T_{fi}^{(\text{post})}(\vec{k}_f, \vec{k}_i) = \langle\Phi_f|V_f|\Psi_i^+\rangle \quad \text{and} \quad T_{fi}^{(\text{prior})}(\vec{k}_f, \vec{k}_i) = \langle\Psi_f^-|V_i|\Phi_i\rangle$$

and hence the the scattering amplitude $A_{fi}(\vec{k}_f, \vec{k}_i)$ is given by

$$A_{fi}(\vec{k}_f, \vec{k}_i) = \left(-\frac{\mu_f}{2\pi}\right)T_{fi}^{(\text{post})}(\vec{k}_f, \vec{k}_i) = \left(-\frac{\mu_f}{2\pi}\right)\langle\Phi_f|V_f|\Psi_i^+\rangle \tag{1}$$

$$= \left(-\frac{\mu_f}{2\pi}\right)T_{fi}^{(\text{prior})}(\vec{k}_f, \vec{k}_i) = \left(-\frac{\mu_f}{2\pi}\right)\langle\Psi_f^-|V_i|\Phi_i\rangle. \tag{2}$$

We now split the interactions V_i and V_f as

$$V_i = U_i + (V_i - U_i) \quad \text{and} \quad V_f = U_f + (V_f - U_f).$$

The distorted-wave method is charaterised by the potential U_i and U_f, called distortion potentials. Judicial approximation of these potentials, which represents the dynamics of the scattering mechanism appropriately produces accurate results. As proposed earlier, we choose the potentials U_i, and U_f, following Bassel and Gerjuoy [24], as

$$U_i = \langle\phi_i|V_i|\phi_i\rangle, \tag{3}$$

$$U_f = \langle\phi_f|V_f|\phi_f\rangle, \tag{4}$$

where ϕ_i, ϕ_f are the bound state wave functions in the initial and final channel, respectively, and the integration is performed over the bound state coordinates. These types of potential basically account for the rearrangement flux property and is most appropriate for rearrangement collisions, because we have neglected the positron-proton interaction. Now when this rearrangement problem is viewed as an inverse scattering problem such that a positronium is incident on a proton the assumption that the positron-proton interaction is negligible is quite natural to get the positron-hydrogen system. However satisfactory results for inelastic collisions are also to be expected by such potentials. With such choices of U_i and U_f it can be easily verified that the effective perturbations $V_i - U_i$ and $V_f - U_f$ are independent of the term $1/r_1$. For instance, for normalized ϕ_i,

$$\begin{aligned} V_i - U_i &= V_2 + V_3 - \langle\phi_i|V_2 + V_3|\phi_i\rangle \\ &= V_2 + V_3 - \langle\phi_i|V_2|\phi_i\rangle - \langle\phi_i|V_3|\phi_i\rangle \\ &= V_2 + V_3 - V_2 - \langle\phi_i|V_3|\phi_i\rangle \\ &= V_3 - \langle\phi_i|V_3|\phi_i\rangle. \end{aligned}$$

With such approximations, the eigenfunctions $|\chi_i^+\rangle, \langle\chi_f^-|$, called, respectively, the "distorted waves" by the potentials U_i and U_f, of $(H_i + U_i), (H_f + U_f)$ satisfy the equations

$$|\chi_i^+\rangle = |\Phi_i\rangle + \frac{1}{E - H_i + i\epsilon}U_i|\chi_i^+\rangle, \tag{5}$$

$$\langle\chi_f^-| = \langle\Phi_f| + \frac{1}{E - H_f + i\epsilon}U_f\langle\chi_f^-|. \tag{6}$$

With some algebraic manipulation it can be shown [36] that the transition matrix elements are expressed in the forms

$$T_{fi}^{(\mathrm{post})}(\vec{k}_f,\vec{k}_i) = \langle \chi_f^- | V_f - U_f | \chi_i^+ \rangle \tag{7}$$

and

$$T_{fi}^{(\mathrm{prior})}(\vec{k}_f,\vec{k}_i) = \langle \chi_f^- | V_i - U_i | \chi_i^+ \rangle . \tag{8}$$

Now replacing χ_i^+ and χ_f^- by Φ_i and Φ_f in Eqs. (5) and (6), respectively, we obtain

$$|\chi_i^+\rangle = |\Phi_i\rangle + \frac{1}{E - H_i + i\epsilon} U_i |\Phi_i\rangle = |\Phi_i\rangle + G_i^+ U_i |\Phi_i\rangle , \tag{9}$$

$$\langle \chi_f^- | = \langle \Phi_f | + \frac{1}{E - H_f + i\epsilon} U_f \langle \Phi_f | = \langle \Phi_f | + G_f^- U_f \langle \Phi_f | , \tag{10}$$

which are then used in the expressions of T_{fi} in Eqs. (7) and (8). Thus our distorted-wave scattering amplitude finally becomes

$$A_{fi}(\vec{k}_f,\vec{k}_i) = \left(-\frac{\mu_f}{2\pi} \right) \langle \chi_f^- | V_f - U_f | \chi_i^+ \rangle \quad \text{(post form)} \tag{11}$$

$$= \left(-\frac{\mu_f}{2\pi} \right) \langle \chi_f^- | V_i - U_i | \chi_i^+ \rangle \quad \text{(prior form)}, \tag{12}$$

where $|\chi_i^+\rangle$ and $\langle \chi_f^-|$ satisfy Eqs. (9) and (10), respectively.

III. APPLICATIONS

A. 1*s*-2*s* excitation of atomic hydrogen by positron impact

Using the prior form of the T-matrix of Eq. (8) we have

$$\begin{aligned} T_{fi}(\vec{k}_f,\vec{k}_i) &= \langle \chi_f^- | V_i - U_i | \chi_i^+ \rangle \\ &= \langle \Phi_f + G_f^- U_f \Phi_f | V_i - U_i | \Phi_i + G_i^+ U_i \Phi_i \rangle \\ &= \langle \Phi_f | V_i | \Phi_i \rangle - \langle \Phi_f | U_i | \Phi_i \rangle + \langle \Phi_f | V_i | G_i^+ U_i \Phi_i \rangle \\ &\quad - \langle \Phi_f | U_i | G_i^+ U_i \Phi_i \rangle + \langle G_f^- U_f \Phi_f | V_i | \Phi_i \rangle \\ &\quad - \langle G_f^- U_f \Phi_f | U_i | \Phi_i \rangle + \langle G_f^- U_f \Phi_f | V_i - U_i | G_i^+ U_i \Phi_i \rangle . \end{aligned} \tag{13}$$

It can be easily verified that making use of post form brings about the same expression. For the case under consideration, we have in a.u.,

$$U_i = \langle \phi_i | V_i | \phi_i \rangle = \langle \phi_{1s} | V_i | \phi_{1s} \rangle = \left(\frac{1}{r_1} + \lambda_i \right) e^{-\beta r_1},$$

$$\begin{aligned} U_f &= \langle \phi_f | V_f | \phi_f \rangle \\ &= \langle \phi_{2s} | V_f | \phi_{2s} \rangle \\ &= \frac{1}{8} (8 + 6\lambda_i r_1 + 2\lambda_i^2 r_1^2 + \lambda_i^3 r_1^3) e^{-\lambda_i r_1}, \end{aligned}$$

where $V_i = V_f = [(1/r_1) - (1/r_{12})]$, $\vec{r}_{12} = \vec{r}_2 - \vec{r}_1$, $\phi_{1s} = \sqrt{\lambda_i^3}/\pi e^{-\lambda_i r_2}$, $\phi_{2s} = 1/\sqrt{32\pi}(2 - \lambda_i r_2) e^{-\lambda_f r_2}$, $\lambda_f = \lambda_i/2$, $\beta = 2\lambda_i$, $\lambda_i = 1$. The plane wave states in the incident and the final channels are given by

$$\Phi_i(\vec{r}_1,\vec{r}_2) = e^{i\vec{k}_i\cdot\vec{r}_1} \phi_{1s}(\vec{r}_2) \quad \text{and} \quad \Phi_f(\vec{r}_1,\vec{r}_2) = e^{i\vec{k}_f\cdot\vec{r}_1} \phi_{2s}(\vec{r}_2) .$$

$\langle \Phi_f | U_i | \Phi_i \rangle$ therefore vanishes due to orthogonality of ϕ_i and ϕ_f.

We now use the bilinear form of Green's function in Eq. (13) as

$$G_i^+(\vec{r}_1,\vec{r}_2;\vec{r}_1{}',\vec{r}_2{}') = \frac{1}{(2\pi)^3} \times \sum_\gamma \int d\vec{k}'' \frac{|\vec{r}_1,\vec{r}_2|\Phi_\gamma''\rangle \; \langle \Phi_\gamma''|\vec{r}_1{}',\vec{r}_2{}'|}{E - E_\gamma'' + i\epsilon} \tag{14}$$

in which the intermediate plane-wave states $|\Phi_\gamma''\rangle$ belong to the incident channel Hamiltonian H_i. In this calculation, we have included only $\gamma = 100$ intermediate state of hydrogen. Thus we have neglected contribution from transition to an intermediate excited state followed by superelastic scattering from that state. We thus obtain

$$\begin{aligned} T_{fi}(\vec{k}_f,\vec{k}_i) &= \langle \Phi_f | V_i | \Phi_i \rangle + \frac{1}{(2\pi)^3} \sum_\gamma \int \frac{d\vec{k}''}{E - E_\gamma'' + i\epsilon} \langle \Phi_f | V_i | \Phi_\gamma'' \rangle \langle \Phi_\gamma'' | U_i | \Phi_i \rangle - \frac{1}{(2\pi)^3} \sum_\gamma \int \frac{d\vec{k}''}{E - E_\gamma'' + i\epsilon} \langle \Phi_f | U_i | \Phi_\gamma'' \rangle \langle \Phi_\gamma'' | U_i | \Phi_i \rangle \\ &\quad + \left(\frac{1}{(2\pi)^3} \sum_\gamma \int \frac{d\vec{k}''}{E - E_\gamma'' + i\epsilon} \langle \Phi_i | V_i | \Phi_\gamma'' \rangle \langle \Phi_\gamma'' | U_f | \Phi_f \rangle \right)^* - \left(\frac{1}{(2\pi)^3} \sum_\gamma \int \frac{d\vec{k}''}{E - E_\gamma'' + i\epsilon} \langle \Phi_i | U_i | \Phi_\gamma'' \rangle \langle \Phi_\gamma'' | U_f | \Phi_f \rangle \right)^* \\ &\quad + \frac{1}{(2\pi)^6} \sum_\gamma \sum_\alpha \int \frac{d\vec{k}''}{E - E_\gamma'' + i\epsilon} \int \frac{d\vec{k}'}{E - E_\alpha' + i\epsilon} \big(\langle \Phi_\gamma'' | V_i - U_i | \Phi_\alpha' \rangle \langle \Phi_\alpha' | U_f | \Phi_f \rangle \big)^* \langle \Phi_\gamma'' | U_i | \Phi_i \rangle \end{aligned} \tag{15}$$

or

TABLE I. The present partial-wave contributions to the $1s$-$2s$ excitation cross section in units of (πa_0^2) of hydrogen atom in e^+-hydrogen collisions in the energy range 20–300 eV. The notation $x[-y]$ stands for $x \times 10^{-y}$. σ includes all significant partial-wave contributions.

	Energy (eV)				
l	20.0	30.0	40.0	54.4	75.0
0	0.1865	0.959[−1]	0.561[−1]	0.305[−1]	0.157[−1]
1	0.761[−1]	0.665[−1]	0.509[−1]	0.349[−1]	0.219[−1]
2	0.188[−1]	0.288[−1]	0.289[−1]	0.248[−1]	0.187[−1]
3	0.322[−2]	0.899[−2]	0.122[−1]	0.134[−1]	0.124[−1]
4	0.439[−3]	0.228[−2]	0.424[−2]	0.608[−2]	0.699[−2]
5	0.519[−4]	0.503[−3]	0.129[−2]	0.243[−2]	0.351[−2]
6	0.557[−5]	0.101[−3]	0.358[−3]	0.888[−3]	0.161[−2]
7		0.188[−4]	0.925[−4]	0.303[−3]	0.697[−3]
8		0.333[−5]	0.227[−4]	0.982[−4]	0.286[−3]
9			0.532[−5]	0.305[−4]	0.113[−3]
10			0.121[−5]	0.917[−5]	0.431[−4]
11				0.268[−5]	0.160[−4]
12					0.580[−5]
13					0.206[−5]
σ	0.2852	0.2031	0.1541	0.1135	0.0821
	Energy (eV)				
l	100.0	150.0	200.0	250.0	300.0
1	0.860[−2]	0.363[−2]	0.197[−2]	0.122[−2]	0.828[−3]
2	0.138[−1]	0.688[−2]	0.407[−2]	0.268[−2]	0.190[−2]
3	0.134[−1]	0.769[−2]	0.493[−2]	0.342[−2]	0.251[−2]
4	0.103[−1]	0.692[−2]	0.485[−2]	0.356[−2]	0.272[−2]
5	0.679[−2]	0.543[−2]	0.418[−2]	0.327[−2]	0.261[−2]
6	0.402[−2]	0.386[−2]	0.330[−2]	0.276[−2]	0.231[−2]
7	0.219[−2]	0.255[−2]	0.243[−2]	0.218[−2]	0.192[−2]
8	0.112[−2]	0.159[−2]	0.170[−2]	0.164[−2]	0.152[−2]
9	0.551[−3]	0.951[−3]	0.114[−2]	0.118[−2]	0.116[−2]
10	0.259[−3]	0.547[−3]	0.734[−3]	0.826[−3]	0.855[−3]
11	0.118[−3]	0.306[−3]	0.461[−3]	0.561[−3]	0.614[−3]
12	0.523[−4]	0.166[−3]	0.282[−3]	0.372[−3]	0.431[−3]
13	0.227[−4]	0.885[−4]	0.169[−3]	0.241[−3]	0.297[−3]
14	0.963[−5]	0.462[−4]	0.997[−4]	0.154[−3]	0.201[−3]
15	0.402[−5]	0.238[−4]	0.578[−4]	0.968[−4]	0.134[−3]
16	0.166[−5]	0.120[−4]	0.330[−4]	0.600[−4]	0.881[−4]
σ	0.0613	0.0407	0.0304	0.0243	0.0202

TABLE II. Present differential cross sections for the $1s$-$2s$ excitation atomic hydrogen by positron impact, in a.u. The notation $x[-y]$ stands for $x \times 10^{-y}$.

Angle (deg)	Energy (eV)				
	20.0	30.0	40.0	75.0	150.0
0	5.14[−1]	6.74[−1]	7.53[−1]	8.63[−1]	9.25[−1]
5	5.04[−1]	6.52[−1]	7.17[−1]	7.80[−1]	7.50[−1]
10	4.77[−1]	5.89[−1]	6.21[−1]	5.83[−1]	4.17[−1]
15	4.35[−1]	5.01[−1]	4.93[−1]	3.71[−1]	1.77[−1]
20	3.85[−1]	4.03[−1]	3.64[−1]	2.99[−1]	6.52[−2]
25	3.31[−1]	3.10[−1]	2.54[−1]	1.10[−1]	2.31[−2]
30	2.77[−1]	2.30[−1]	1.70[−1]	5.62[−2]	8.65[−3]
35	2.28[−1]	1.67[−1]	1.11[−1]	2.89[−2]	3.64[−3]
40	1.85[−1]	1.19[−1]	7.22[−1]	1.55[−2]	1.78[−3]
45	1.48[−1]	8.50[−2]	4.73[−2]	8.81[−3]	1.00[−3]
50	1.18[−1]	6.10[−2]	3.17[−2]	5.41[−3]	6.31[−4]
55	9.47[−2]	4.43[−2]	2.18[−2]	3.57[−3]	4.29[−4]
60	7.61[−2]	3.29[−2]	1.56[−2]	2.51[−3]	3.08[−4]
65	6.16[−2]	2.50[−2]	1.16[−2]	1.86[−3]	2.29[−4]
70	5.04[−2]	1.94[−2]	8.89[−2]	1.43[−3]	1.76[−4]
75	4.17[−2]	1.55[−2]	7.05[−3]	1.14[−3]	1.38[−4]
80	3.51[−2]	1.27[−2]	5.75[−3]	9.24[−4]	1.10[−4]
85	2.99[−2]	1.06[−2]	4.80[−3]	7.64[−4]	9.00[−5]
90	2.58[−2]	9.09[−3]	4.08[−3]	6.43[−4]	7.50[−5]
95	2.26[−2]	7.88[−3]	3.53[−3]	5.48[−4]	6.30[−5]
100	2.01[−2]	6.94[−3]	3.10[−3]	4.73[−4]	5.40[−5]
105	1.80[−2]	6.19[−3]	2.75[−3]	4.13[−4]	4.60[−5]
110	1.64[−2]	5.58[−3]	2.46[−3]	3.65[−4]	4.00[−5]
115	1.50[−2]	5.09[−3]	2.23[−3]	3.25[−4]	3.60[−5]
120	1.39[−2]	4.68[−3]	2.04[−3]	2.93[−4]	3.20[−5]
125	1.29[−2]	4.33[−3]	1.87[−3]	2.66[−4]	2.90[−5]
130	1.22[−2]	4.05[−3]	1.74[−3]	2.44[−4]	2.70[−5]
135	1.15[−2]	3.81[−3]	1.63[−3]	2.26[−4]	2.40[−5]
140	1.10[−2]	3.61[−3]	1.53[−3]	2.11[−4]	2.30[−5]
145	1.05[−2]	3.44[−3]	1.46[−3]	1.99[−4]	2.10[−5]
150	1.02[−2]	3.30[−3]	1.39[−3]	1.89[−4]	2.00[−5]
155	9.86[−3]	3.19[−3]	1.34[−3]	1.81[−4]	1.90[−5]
160	9.62[−3]	3.11[−3]	1.30[−3]	1.75[−4]	1.90[−5]
165	9.44[−3]	3.04[−3]	1.27[−3]	1.70[−4]	1.80[−5]
170	9.32[−3]	2.99[−3]	1.25[−3]	1.67[−4]	1.80[−5]
175	9.24[−3]	2.96[−3]	1.24[−3]	1.65[−4]	1.80[−5]
180	9.22[−3]	2.96[−3]	1.23[−3]	1.64[−4]	1.80[−5]

$$T_{fi}(\vec{k}_f,\vec{k}_i) = \langle \Phi_f | V_i | \Phi_i \rangle + \frac{1}{(2\pi)^3} \sum_{\gamma} \int \frac{d\vec{k}''}{E - E''_{\gamma} + i\epsilon} \langle \Phi_f | V_i | \Phi''_{\gamma} \rangle \times \langle \Phi''_{\gamma} | U_i | \Phi_i \rangle, \tag{16}$$

where *denotes the complex conjugate of the respective terms in angle brackets and the last four terms of Eq. (15) vanish due to the orthogonality of hydrogenic states. It is to be noted that the appearance of the residual interaction V_i in Eqs. (15) and (16) is an outcome of splitting $V_i - U_i$ as in Eq. (13). That $V_i - U_i$ does not involve the positron-proton interaction is explained below Eq. (4).

Now using the relations of the amplitudes such as

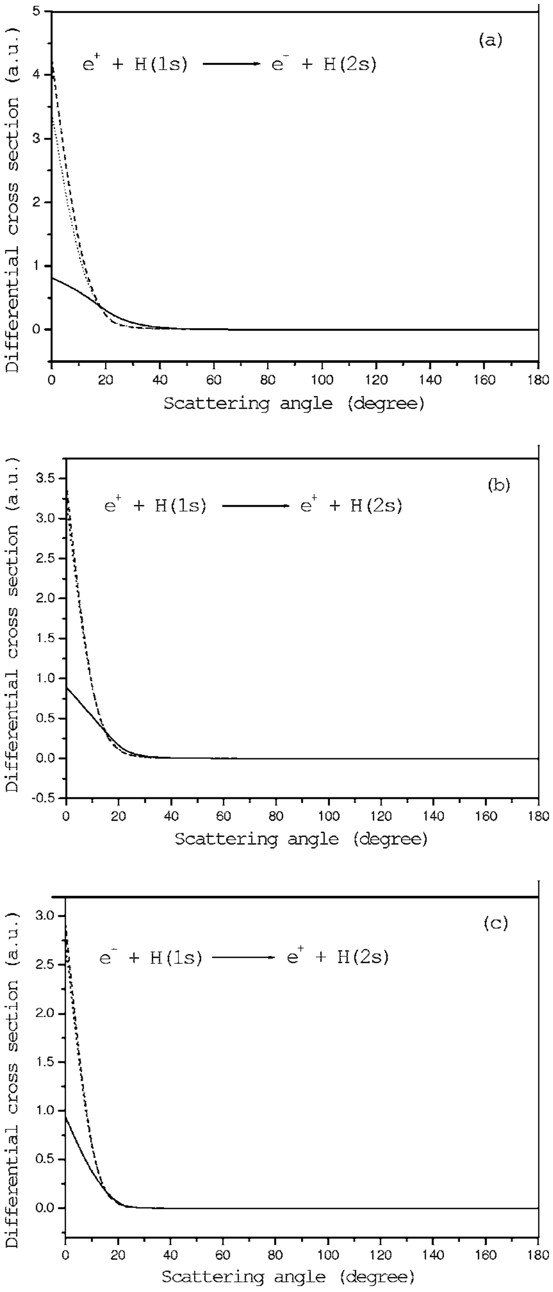

FIG. 2. Differential cross section for $e^{+}+\mathrm{H}(1s)\rightarrow e^{+}+\mathrm{H}(2s)$ at (a) 54.4 eV, (b) 100.0 eV, and (c) 200.0 eV. Solid line, present results; dashed line, cross sections, Ref. [32]; dotted line, DWB2D, Ref. [30].

$$g_B(\vec{k}_f,\vec{k}_i)=\left(-\frac{2\pi}{\mu_f}\right)^{-1}\langle\Phi_f|V_i|\Phi_i\rangle,\quad f_{f\gamma}(\vec{k}_f,\vec{k}_i)=\left(-\frac{2\pi}{\mu_\gamma}\right)^{-1}\langle\Phi_f|V_i|\Phi''_\gamma\rangle,\quad \text{etc.},$$

we obtain from Eq. (16),

$$A_{fi}(\vec{k}_f,\vec{k}_i)=g_B(\vec{k}_f,\vec{k}_i)+D_{fi}(\vec{k}_f,\vec{k}_i), \tag{17}$$

where

TABLE III. Integrated cross section for $e^{+}+\mathrm{H}(1s)\rightarrow e^{+}+\mathrm{H}(2s)$, in units of πa_0^2.

Energy (eV)	54.4	100.0	200.0	300.0
Present	0.1135	0.0613	0.0304	0.0202
CCPA[a]	0.127	0.061	0.030	0.020
UEBS1[b]		0.061	0.030	
CCOM[c]	0.124	0.080	0.040	
Pseudomodel[d]	0.072	0.049	0.027	
21-state CCA[e]	0.126			
First Born	0.102	0.058	0.030	0.020

[a] CCPA, close-coupled pseudostate approximation by Walters [32].

[b] UEBS1, unitarized eikonal-Born series (version 1), Byron *et al.* [33].

[c] CCOM, coupled-channel optical model, Bransden *et al.* [34].

[d] Pseudomodel by Mukherjee *et al.* [39].

[e] 21-state close coupling approximation, Morgan [35].

$$D_{fi}(\vec{k}_f,\vec{k}_i)=\frac{1}{(2\pi)^3}\sum_\gamma\left(-\frac{2\pi}{\mu_\gamma}\right)\times\int\frac{d\vec{k}''}{E-E''_\gamma+i\epsilon}f_{f\gamma}(\vec{k}_f,\vec{k}_i)f_{\gamma i}(\vec{k}_f,\vec{k}_i). \tag{18}$$

It is not convenient to evaluate the amplitude (17) as a function of the scattering angle in threedimensions. We would rather perform the partial-wave analysis on this amplitude to reduce it to a form amenable for computations by expanding both sides of Eq. (17) as

$$A_{fi}(\vec{k}_f,\vec{k}_i)=\frac{4\pi}{\sqrt{k_ik_f}}\sum_{l,m}A^{l}_{fi}(k_f,k_i)Y_{lm}(\hat{k}_f)Y^{*}_{lm}(\hat{k}_i), \tag{19}$$

$$g_B(\vec{k}_f,\vec{k}_i)=\frac{4\pi}{\sqrt{k_ik_f}}\sum_{l,m}g^{l}_{B}(k_f,k_i)Y_{lm}(\hat{k}_f)Y^{*}_{lm}(\hat{k}_i), \tag{20}$$

and similarly for the other amplitudes. On multiplication with $Y^{*}_{L0}(\hat{k}_f)$ and integration over $\hat{k}_f$, one obtains with using

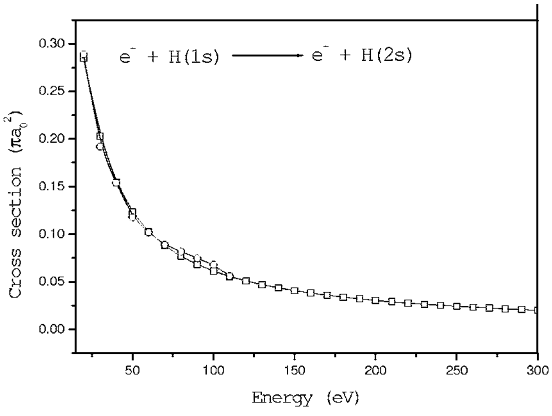

FIG. 3. Total $1s$-$2s$ excitation cross section of hydrogen atom in positron-hydrogen collisions in the energy range 20–300 eV. Open square, present results; open circle, Kernohgan *et al.* [41]

TABLE IV. Present partial-wave contributions to the ground state Ps formation cross section in units of (πa_0^2) in e^+-hydrogen collisions in the energy range 20–300 eV. The notation $x[-y]$ stands for $x \times 10^{-y}$ includes all significant partial-wave contributions.

	Energy (eV)				
l	20.0	25.0	35.0	50.0	75.0
0	0.9862	0.4981	0.1782	0.5674[−1]	0.1373[−1]
1	0.2138	0.1183	0.4090[−1]	0.1130[−1]	0.2275[−2]
2	0.8562	0.5298	0.2133	0.6764[−1]	0.1528[−1]
3	0.7875	0.5661	0.2694	0.9638[−1]	0.2374[−1]
4	0.4642	0.3898	0.2206	0.8971[−1]	0.2431[−1]
5	0.2189	0.2149	0.1449	0.6717[−1]	0.2013[−1]
6	0.9008[−1]	0.1034	0.8314[−1]	0.4397[−1]	0.1461[−1]
7	0.3377[−1]	0.4531[−1]	0.4347[−1]	0.2626[−1]	0.9691[−2]
8	0.1182[−1]	0.1855[−1]	0.2124[−1]	0.1467[−1]	0.6016[−2]
9	0.3926[−2]	0.7208[−2]	0.9850[−2]	0.7778[−2]	0.3550[−2]
10	0.1251[−2]	0.2686[−2]	0.4383[−2]	0.3960[−2]	0.2012[−2]
11	0.3850[−3]	0.9677[−3]	0.1886[−2]	0.1950[−2]	0.1104[−2]
12	0.1152[−3]	0.3389[−3]	0.7889[−3]	0.9339[−3]	0.5889[−3]
13	0.3365[−4]	0.1159[−3]	0.3223[−3]	0.4369[−3]	0.3070[−3]
14	0.9630[−5]	0.3880[−4]	0.1290[−3]	0.2003[−3]	0.1569[−3]
σ	3.6682	2.4956	1.2327	4.8912[−1]	1.3764[−1]

	Energy (eV)				
l	100.0	150.0	200.0	250.0	300.0
0	0.4610[−2]	0.8749[−3]	0.2463[−3]	0.8765[−4]	0.3647[−4]
1	0.6801[−3]	0.1137[−3]	0.3017[−4]	0.1046[−4]	0.4332[−5]
2	0.4813[−2]	0.8334[−3]	0.2216[−3]	0.7610[−4]	0.3101[−4]
3	0.7754[−2]	0.1380[−2]	0.3698[−3]	0.1272[−3]	0.5181[−4]
4	0.8299[−2]	0.1535[−2]	0.4180[−3]	0.1449[−3]	0.5923[−4]
5	0.7214[−2]	0.1397[−2]	0.3882[−3]	0.1361[−3]	0.5600[−4]
6	0.5512[−2]	0.1122[−2]	0.3191[−3]	0.1133[−3]	0.4703[−4]
7	0.3854[−2]	0.8261[−3]	0.2410[−3]	0.8686[−4]	0.3638[−4]
8	0.2524[−2]	0.5710[−3]	0.1711[−3]	0.6260[−4]	0.2649[−4]
9	0.1573[−2]	0.3757[−3]	0.1157[−3]	0.4303[−4]	0.1840[−4]
10	0.9416[−3]	0.2378[−3]	0.7527[−4]	0.2847[−4]	0.1231[−4]
11	0.5458[−3]	0.1458[−3]	0.4747[−4]	0.1825[−4]	0.7981[−5]
12	0.3078[−3]	0.8702[−4]	0.2915[−4]	0.1140[−4]	0.5042[−5]
13	0.1697[−3]	0.5076[−4]	0.1750[−4]	0.6966[−5]	0.3116[−5]
14	0.9169[−4]	0.2902[−4]	0.1030[−4]	0.4172[−5]	0.1888[−5]
σ	4.8977[−2]	9.6092[−3]	2.7119[−3]	9.6213[−4]	3.9964[−4]

the orthogonal properties of the spherical harmonicss,

$$\int Y^*_{L0}(\hat{k}_f)[A_{fi}(\vec{k}_f,\vec{k}_i)]d\hat{k}_f = \frac{4\pi}{\sqrt{k_f k_i}}[A^{(L)}_{fi}(k_f,k_i)]Y^*_{L0}(\hat{k}_i), \tag{21}$$

and similar other expressions. On choosing the direction of incidence along the Z axis, one has $\vec{k}_i=(0,0,k_i), \hat{k}_i . \hat{k}_f = \cos\theta_f, \hat{Y}_{L0}(\hat{k}_f) = \sqrt{(2L+1)/4\pi}P_L(\cos\theta_f) d\hat{k}_f = \sin\theta_f d\theta_f d\phi_f$, thus on integration over ϕ_f, the partial-wave scattering amplitude is obtained as

$$[A^{(L)}_{fi}(k_f,\, k_i)] = \sqrt{k_i k_f}/2\int_{-1}^{+1}[A_{fi}(\vec{k}_f,\vec{k}_i)]P_L(\cos\theta_f)d(\cos\theta_f). \tag{22}$$

Other amplitudes are all analyzed similarly. In order to perform the partial-wave analysis of the amplitude involving the

TABLE V. Present partial-wave contributions to the Ps(2s) and Ps(3s) formation cross section in units of (πa_0^2) in e^+-hydrogen collisions in the energy range 20–300 eV. The notation $x[-y]$ stands for $x \times 10^{-y}$. σ includes all significant partial-wave contributions.

Reaction: $e^+ + \mathrm{H}(1s) \rightarrow \mathrm{Ps}(2s) + \mathrm{H}^+$

	Energy (eV)					
l	20.0	50.0	75.0	100.0	200.0	300.0
0	0.2130	0.8360[−2]	0.1971[−2]	0.6503[−3]	0.3304[−4]	0.4480[−5]
1	0.7882[−2]	0.1338[−2]	0.2781[−3]	0.8429[−4]	0.4042[−5]	0.6726[−6]
2	0.6038[−1]	0.9393[−2]	0.2167[−2]	0.6801[−3]	0.3225[−4]	0.4419[−5]
3	0.4733[−1]	0.1366[−1]	0.3493[−2]	0.1140[−2]	0.5401[−4]	0.7356[−5]
4	0.2189[−1]	0.1274[−1]	0.3600[−2]	0.1232[−2]	0.5971[−4]	0.8337[−5]
5	0.7920[−2]	0.9441[−2]	0.3040[−2]	0.1089[−2]	0.5524[−4]	0.7918[−5]
6	0.2478[−2]	0.6179[−2]	0.2197[−2]	0.8311[−3]	0.4663[−4]	0.6704[−5]
7	0.7019[−3]	0.3591[−2]	0.1499[−2]	0.5996[−3]	0.3592[−4]	0.5292[−5]
8	0.1846[−3]	0.2025[−2]	0.9161[−3]	0.3939[−3]	0.2537[−4]	0.3853[−5]
9	0.4576[−4]	0.1027[−2]	0.5471[−3]	0.2503[−3]	0.1746[−4]	0.2609[−5]
10	0.1079[−4]	0.5268[−3]	0.3110[−3]	0.1464[−3]	0.1174[−4]	0.1734[−5]
11	0.2438[−5]	0.2563[−3]	0.1679[−3]	0.8434[−4]	0.7197[−5]	0.1176[−5]
12		0.1123[−3]	0.9803[−4]	0.5254[−4]	0.4240[−5]	
13		0.5857[−4]	0.4378[−4]	0.2728[−4]	0.2733[−5]	
14		0.2276[−4]	0.2399[−4]	0.1509[−4]	0.1667[−5]	
σ	3.6178[−1]	6.8746[−2]	2.0375[−2]	7.2910[−3]	3.9307[−4]	5.6380[−5]

Reaction: $e^+ + \mathrm{H}(1s) \rightarrow \mathrm{Ps}(3s) + \mathrm{H}^+$

	Energy (eV)					
l	20.0	50.0	75.0	100.0	200.0	300.0
0	0.2667[−1]	0.2893[−2]	0.7838[−3]	0.2668[−3]	0.9430[−5]	0.1040[−5]
1	0.5381[−2]	0.2825[−3]	0.4647[−4]	0.1184[−4]	0.1460[−5]	0.4100[−6]
2	0.1738[−1]	0.2716[−2]	0.5546[−3]	0.1751[−3]	0.9300[−5]	0.1679[−5]
3	0.1155[−1]	0.3861[−2]	0.9444[−3]	0.3055[−3]	0.1545[−4]	0.2508[−5]
4	0.4781[−2]	0.3786[−2]	0.1071[−2]	0.3554[−3]	0.1844[−4]	0.2740[−5]
5	0.1574[−2]	0.2780[−2]	0.9290[−3]	0.3295[−3]	0.1781[−4]	0.2517[−5]
6	0.4511[−3]	0.1837[−2]	0.6882[−3]	0.2646[−3]	0.1453[−4]	0.2100[−5]
7	0.1175[−3]	0.1082[−2]	0.4044[−3]	0.1714[−3]	0.1075[−4]	0.1618[−5]
8	0.2850[−4]	0.5436[−3]	0.2745[−3]	0.1137[−3]	0.7790[−5]	0.1168[−5]
9	0.6550[−5]	0.3639[−3]	0.1681[−3]	0.6805[−4]	0.5257[−5]	
10	0.1420[−5]	0.1293[−3]	0.1149[−3]	0.5280[−4]	0.3398[−5]	
11		0.8010[−4]	0.5087[−4]	0.3430[−4]	0.2279[−5]	
12		0.3464[−4]	0.1478[−4]	0.1185[−4]	0.1550[−5]	
13		0.1233[−4]	0.2208[−4]	0.5860[−5]		
14		0.1726[−4]	0.9230[−5]	0.3890[−5]		
σ	6.7938[−2]	2.0431[−2]	6.0812[−3]	2.1775[−3]	1.1923[−4]	1.8110[−4]

pole term $1/(E-E''_\gamma \pm i\epsilon)$, we split it into a δ-function part and a principal-value part,

$$1/(E - E''_\gamma \pm i\epsilon) = \mp i\pi\delta(E - E''_\gamma) + \mathrm{P}\frac{1}{E - E''_\gamma}. \qquad (23)$$

We thus get $D_{fi}(\vec{k}_f,\vec{k}_i)$ as

$$\begin{aligned} D_{fi}^{(L)}(k_f, k_i) &= i\sum_\gamma f_{f\gamma}^{(L)}(k_f, k_\gamma) f_{\gamma i}^{(L)}(k_\gamma,k_i) \\ &\quad - \frac{2}{\pi}\sum_\gamma \mathrm{P}\int_0^\infty \frac{k''dk''}{k_\gamma^2 - k''^2} f_{f\gamma}^{(L)}(k_f, k'') f_{\gamma i}^{(L)}(k'', k_i) \\ &= (D_{fi}^{(r)}, D_{fi}^{(i)}). \end{aligned} \qquad (24)$$

TABLE VI. Present differential cross sections (a.u.) for the reactions $e^{+}+\mathrm{H}(1s)\rightarrow\mathrm{Ps}(n's)+p$. The notation $x[-y]$ stands for $x\times10^{-y}$.

Reactions	$e^{+}+\mathrm{H}(1s)\rightarrow\mathrm{Ps}(1s)+p$		$e^{+}+\mathrm{H}(1s)\rightarrow\mathrm{Ps}(2s)+p$		$e^{+}+\mathrm{H}(1s)\rightarrow\mathrm{Ps}(3s)+p$	
Angle (deg)	50 eV	100 eV	50 eV	100 eV	50 eV	100 eV
0.0	0.1023[2]	0.1459[1]	0.1394[1]	0.2238	0.4036	0.6500[−1]
5.0	0.8234[1]	0.1086[1]	0.1128[1]	0.1655	0.3259	0.4769[−1]
10.0	0.4335[1]	0.4567	0.6002	0.6836[−1]	0.1723	0.1912[−1]
15.0	0.1490[1]	0.1087	0.2084	0.1568[−1]	0.5872[−1]	0.4044[−2]
20.0	0.2962	0.1048[−1]	0.4132[−1]	0.1360[−2]	0.1101[−1]	0.2440[−3]
25.0	0.1250[−1]	0.3190[−3]	0.1567[−2]	0.8100[−4]	0.2800[−3]	0.7800[−4]
30.0	0.1705[−1]	0.5026[−2]	0.2770[−2]	0.8300[−3]	0.1140[−2]	0.3650[−3]
35.0	0.6026[−1]	0.8039[−2]	0.9325[−2]	0.1254[−2]	0.3255[−2]	0.4930[−3]
40.0	0.8422[−1]	0.8546[−2]	0.1289[−1]	0.1297[−2]	0.4320[−2]	0.4880[−3]
45.0	0.8896[−1]	0.7842[−2]	0.1353[−1]	0.1169[−2]	0.4454[−2]	0.4310[−3]
50.0	0.8342[−1]	0.6786[−2]	0.1261[−1]	0.9980[−3]	0.4113[−2]	0.3610[−3]
55.0	0.7406[−1]	0.5750[−2]	0.1113[−1]	0.8350[−3]	0.3607[−2]	0.2980[−3]
60.0	0.6421[−1]	0.4856[−2]	0.9593[−2]	0.6980[−3]	0.3095[−2]	0.2310[−3]
65.0	0.5527[−1]	0.4124[−2]	0.8200[−2]	0.5960[−3]	0.2638[−2]	0.1630[−3]
70.0	0.4763[−1]	0.3534[−2]	0.7018[−2]	0.5010[−3]	0.2252[−2]	0.2000[−3]
75.0	0.4130[−1]	0.3062[−2]	0.6042[−2]	0.4190[−3]	0.1936[−2]	0.1740[−3]
80.0	0.3612[−1]	0.2681[−2]	0.5245[−2]	0.3920[−3]	0.1667[−2]	0.1030[−3]
85.0	0.3189[−1]	0.2373[−2]	0.4601[−2]	0.3110[−3]	0.1501[−2]	0.1610[−3]
90.0	0.2843[−1]	0.2122[−2]	0.4064[−2]	0.3120[−3]	0.1346[−2]	0.8000[−4]
95.0	0.2559[−1]	0.1915[−2]	0.3657[−2]	0.2460[−3]	0.1055[−2]	0.1150[−3]
100.0	0.2324[−1]	0.1743[−2]	0.3257[−2]	0.2490[−3]	0.1148[−2]	0.7500[−4]
105.0	0.2129[−1]	0.1600[−2]	0.3026[−2]	0.2200[−3]	0.9820[−3]	0.6300[−4]
110.0	0.1965[−1]	0.1479[−2]	0.2747[−2]	0.1870[−3]	0.6710[−3]	0.1000[−3]
115.0	0.1828[−1]	0.1377[−2]	0.2486[−2]	0.2010[−3]	0.1106[−2]	0.5400[−4]
120.0	0.1713[−1]	0.1291[−2]	0.2422[−2]	0.1740[−3]	0.7780[−3]	0.5100[−4]
125.0	0.1614[−1]	0.1218[−2]	0.2282[−2]	0.1490[−3]	0.4950[−3]	0.8200[−4]
130.0	0.1532[−1]	0.1155[−2]	0.2047[−2]	0.1600[−3]	0.6210[−3]	0.5100[−4]
135.0	0.1461[−1]	0.1103[−2]	0.1920[−2]	0.1600[−3]	0.9230[−3]	0.4200[−4]
140.0	0.1402[−1]	0.1058[−2]	0.1921[−2]	0.1400[−3]	0.7820[−3]	0.4100[−4]
145.0	0.1353[−1]	0.1020[−2]	0.1930[−2]	0.1240[−3]	0.5190[−3]	0.5800[−4]
150.0	0.1311[−1]	0.9890[−3]	0.1876[−2]	0.1230[−3]	0.4120[−3]	0.6200[−4]
155.0	0.1278[−1]	0.9630[−3]	0.1779[−2]	0.1290[−3]	0.3890[−3]	0.4600[−4]
160.0	0.1251[−1]	0.9430[−3]	0.1682[−2]	0.1330[−3]	0.4110[−3]	0.3800[−4]
165.0	0.1231[−1]	0.9280[−3]	0.1609[−2]	0.1340[−3]	0.4610[−3]	0.3500[−4]
170.0	0.1217[−1]	0.9170[−3]	0.1565[−2]	0.1320[−3]	0.5190[−3]	0.3400[−4]
175.0	0.1209[−1]	0.9110[−3]	0.1542[−2]	0.1310[−3]	0.5610[−3]	0.3300[−4]
180.0	0.1206[−1]	0.9090[−3]	0.1536[−2]	0.1300[−3]	0.5760[−3]	0.3300[−4]

In terms of these amplitudes, the partial-wave form of the distorted wave amplitude is given as

$$A_{fi}^{(L)}(k_f,\,k_i)=g_B^{(L)}(k_f,\,k_i)+D_{fi}^{(L)}(k_f,\,k_i) \tag{25}$$

which is a function of the scattering energies for any partial wave L.

1. Results and discussion:

We have calculated the distorted-wave amplitudes for $1s$-$2s$ excitation using the relation (25). The evaluation of the single-dimensional principal-value integral over $[0,\infty)$ can be performed quite accurately by splitting the range into intervals $[0,2k_\gamma]$ and $[2k_\gamma,\infty)$. Then we use Gauss Legendre quadrature of even number of points for the first interval $[0,2k_\gamma]$ such that the principal-value integral is defined characteristically as

TABLE VII. Differential cross sections (a.u.) as a function of scattering angle for the reaction $e^{+}+\mathrm{H}(1s)\rightarrow\mathrm{Ps}(1s)+\mathrm{H}^{+}$. The notation $x[-y]$ stands for $x\times10^{-y}$.

Angle (deg)	Energy (20 eV)				
	DWA[a]	JS[b]	SW[c]	MGS[d]	MG[e]
0	2.9[1]	3.2[1]	4.2[1]	4.0[1]	4.1[1]
5	2.6[1]	2.9[1]	3.8[1]	3.6[1]	3.7[1]
10	1.8[1]	2.1[1]	2.8[1]	2.7[1]	2.8[1]
15	1.0[1]	1.2[1]	1.8[1]	1.7[1]	1.7[1]
20	4.3	5.5	9.3	8.8	9.2
25	1.2	1.9	4.0	3.8	4.1
30	1.3[−1]	3.5[−1]	1.3	1.4	1.5
35	5.8[−2]	1.2[−3]	5.3[−2]	3.7[−1]	4.5[−1]
40	3.2[−1]	1.1[−1]	−3.8[−1]	5.8[−2]	8.0[−2]
	Energy (200 eV)				
0	9.8[−2]	1.0[−1]	1.2[−1]	1.3[−1]	1.4[−1]
5	6.9[−2]	7.1[−2]	8.9[−2]	9.8[−2]	1.0[−1]
10	2.4[−2]	2.6[−2]	3.6[−2]	4.2[−2]	4.3[−2]
15	4.4[−3]	5.1[−3]	9.2[−3]	1.3[−2]	1.3[−2]
20	2.2[−4]	3.6[−4]	1.4[−3]	3.2[−3]	3.1[−3]
25	9.9[−5]	2.7[−5]	-2.1[−4]	8.0[−4]	7.3[−4]

[a] Present calculation.
[b] Reference [43].
[c] Reference [27].
[d] Reference [25]
[e] Reference [26].

$$\lim_{\delta\to0^{+}}\left(\int_{0}^{k_{\gamma}-\delta}dk''\cdots+\int_{k_{\gamma}+\delta}^{2k_{\gamma}}dk''\cdots\right),$$

since the distribution of quadrature points are evenly distributed around the midpoint $k''=k_{\gamma}$. The evaluation of the integral for the other interval $[2k_{\gamma},\infty)$ can be performed in a straightforward manner by using any standard technique. We have however used the Gauss-Legendre method with 20 quadrature points for smooth convergence of the results.

The results of present partial-wave contributions to the $1s$-$2s$ excitation cross section of hydrogen atom in e^{+}-hydrogen collisions have been presented in Table I in the energy range 20–300 eV. We have included all the significant partial wave contributions to calculate total cross section. It is clear from Table I that the contribution of partial waves to the total cross section decreases monotonically with the higher partial waves. It clearly indicates that, as we shall see later, critical angles in the differential cross section do not move in the forward direction and hence there exists no secondary maxima or minima. Critical angles are defined to be those scattering angles at which differential cross section assumes its minimum value for a perticular incident positron energy (existence and behavior of critical angle along with the secondary maxima and minima for positron-hydrogen collisions have been studied in detailed in Refs. [48–50]. To be more precise, the steadily decreasing partial wave contribution implies that the scattering amplitudes are of the same nature, and this steadily decreasing amplitudes, by which the differential cross section is calculated, can not introduce some up and down structures in the differential cross section. These results of distorted-wave theory have been used to compute the differential cross section as a function of scattering angle and energy. We have approximated the higher partial wave contribution to the distorted wave amplitudes by the corresponding FBA values so that the differential cross section for $1s$-$2s$ excitation of hydrogen atom by positron impact takes the form

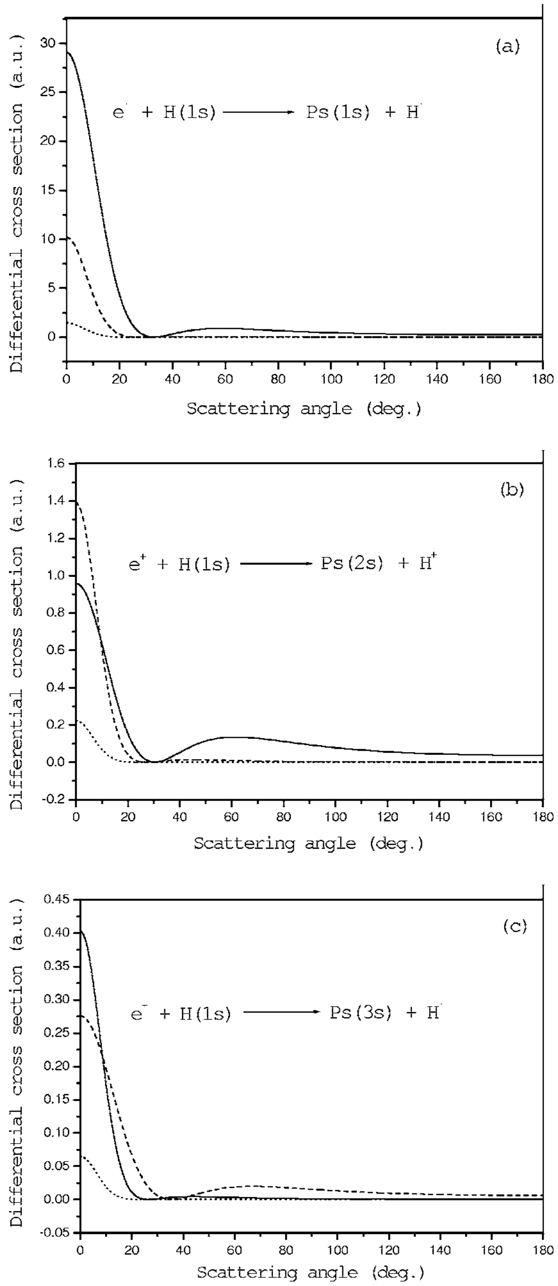

FIG. 4. Differential cross section (a.u.) as a function of scattering angle (in degrees) for the reactions (a) $e^{+}+\mathrm{H}(1s)\rightarrow\mathrm{Ps}(1s)+H^{+}$, $(b)e^{+}+\mathrm{H}(1s)\rightarrow\mathrm{Ps}(2s)+H^{+}$, and (c) $e^{+}+\mathrm{H}(1s)\rightarrow\mathrm{Ps}(3s)+H^{+}$ at the energies 20 eV, 50 eV, and 100 eV, respectively, solid line, 20 eV; dashed line, 50 eV; dotted line, 100 eV.

$$\frac{d\sigma}{d\Omega} = \frac{k_f}{k_i}|A_{fi}(\vec{k}_f, \vec{k}_i)|^2 = \frac{k_f}{k_i}|A_r(\vec{k}_f, \vec{k}_i)|^2 + |A_i(\vec{k}_f, \vec{k}_i)|^2, \tag{26}$$

where

$$\begin{aligned} A_r(\vec{k}_f, \vec{k}_i) &= \frac{1}{\sqrt{k_i k_f}}\sum_{l=0}^{\infty}(2l+1)A_r^{(l)}(k_f, k_i)P_l(\cos\theta) \\ &= \frac{1}{\sqrt{k_i k_f}}\left(\sum_{l=0}^{L}(2l+1)A_r^{(l)}(k_f, k_i)P_l(\cos\theta) \right. \\ &\quad \left. + \sum_{l=L+1}^{\infty}(2l+1)g_B^{(l)}(k_f, k_i)P_l(\cos\theta)\right) \\ &= \frac{1}{\sqrt{k_i k_f}}\sum_{l=0}^{L}(2l+1)\left[A_r^{(l)}(k_f, k_i) - g_B^{(l)}(k_f, k_i)\right] \\ &\quad \times P_l(\cos\theta) + g_B(\vec{k}_f, \vec{k}_i) \end{aligned} \tag{27}$$

and

$$\begin{aligned} A_i(\vec{k}_f, \vec{k}_i) &= \frac{1}{\sqrt{k_i k_f}}\sum_{l=0}^{\infty}(2l+1)A_i^{(l)}(k_f, k_i)P_l(\cos\theta) \\ &= \frac{1}{\sqrt{k_i k_f}}\sum_{l=0}^{L}(2l+1)A_i^{(l)}(k_f, k_i)P_l(\cos\theta). \end{aligned} \tag{28}$$

L is the number of partial waves up to which the contribution of distorted-wave amplitudes have been taken into account. The accuracy of the values of differential cross sections has been examined by integrating the differential cross sections over the entire solid angle to obtain the total cross section

$$\sigma = 2\int_{-1}^{1}\left(\frac{d\sigma}{d\Omega}\right)d(\cos\theta) \quad (\text{units of } \pi a_0^2). \tag{29}$$

This formula (29) reproduces the same results for total cross sections as obtained by summing up the partial-wave contribution.

Our presents results of differential cross sections for the 1s-2s excitation of atomic hydrogen by positron impact have been displayed in Table II at some discrete energies in the range 20–150 eV. It is clear that forward scattering dominates over the backward scattering. Cross section peaks at the very forward angles and then slowly decreases to become nearly flat at the backward scattering angles. Hence critical angle always lies at the backward extremity (180°) of the scattering angle and consequently no secondary minima or maxima appears in the curve of differential cross sections. In Fig. 2 we have compared our results of differential cross sections at the incident energies 54.4 eV, 100.0 eV, and 200.0 eV, respectively, with those of Walters [32] and of Bubelev *et al.* [30]. The present results near the forward angles are always less than those of the other predictions. Except below the scattering angle 150°, the present results coincidence with those of Walters [32] and Bubelev *et al.* [30]. It is a matter of fact that the results of different theoretical calculations differ considerably very near the forward directions [30–32,39,40]. With the increase in energy the difference between the different theoretical predictions decreases. We believe that present results at intermediate and large scattering angles are expected to be reliable since the calculation is devised to approximate the rearrangement channel, which is responsible for important short-range correlations. The inability of the present method to account for the loss of inelastic flux appropriately is responsible for the discrepancies near the forward directions. Proper approximation of the discrete and continuum intermediate states by the distortion potential will accurately present the differential cross sections near the forward directions, we believe. Our integrated in-

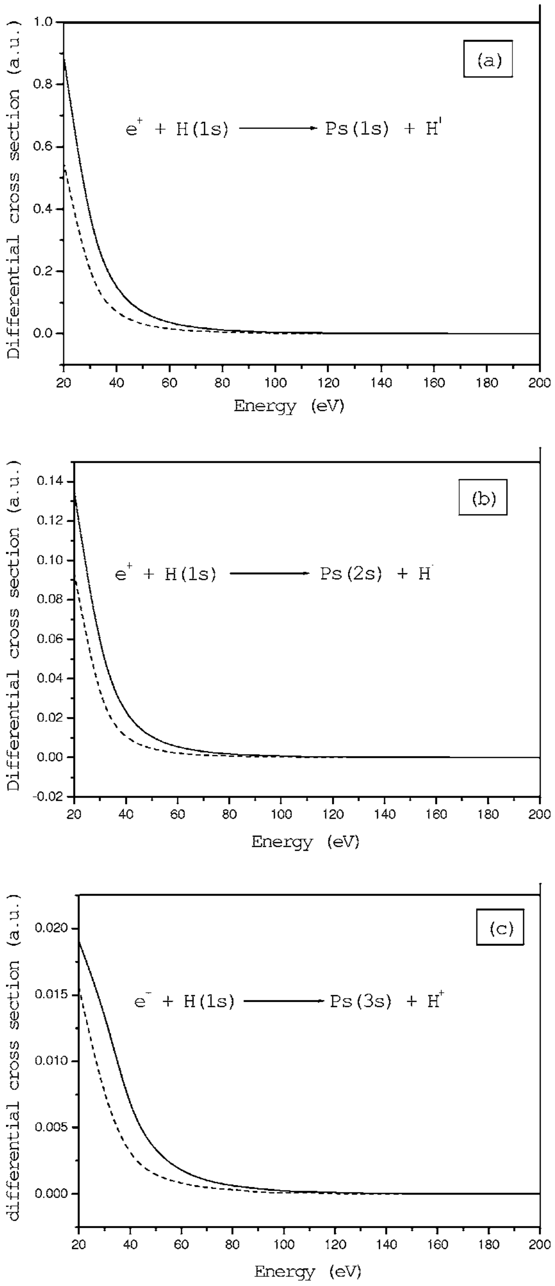

FIG. 5. Differential cross section (a.u.) as a function of energy (in eV) for the reactions (a) $e^+ + \mathrm{H}(1s) \rightarrow \mathrm{Ps}(1s) + \mathrm{H}^+$, (b) $e^+ + \mathrm{H}(1s) \rightarrow \mathrm{Ps}(2s) + \mathrm{H}^+$, and (c) $e^+ + \mathrm{H}(1s) \rightarrow \mathrm{Ps}(3s) + \mathrm{H}^+$ for the angle 60° and 90°, respectively, solid line, 60° dashed line, 90°.

TABLE VIII. Critical angles θ_c along with the differential cross sections $(d\sigma/d\Omega)_{\theta_c}$ for the reactions $e^+ + \mathrm{H}(1s) \to \mathrm{Ps}(n's) + p$ in the energy range $E \in [20, 150]$. The notation $x[-y]$ stands for $x \times 10^{-y}$.

Reactions	$e^+ + \mathrm{H}(1s) \to \mathrm{Ps}(1s) + p$		$e^+ + \mathrm{H}(1s) \to \mathrm{Ps}(2s) + p$		$e^+ + \mathrm{H}(1s) \to \mathrm{Ps}(3s) + p$	
E(eV)	θ_c(deg)	$(d\sigma/d\Omega)_{\theta_c}$ (a.u.)	θ_c(deg)	$(d\sigma/d\Omega)_{\theta_c}$ (a.u.)	θ_c(deg)	$(d\sigma/d\Omega)_{\theta_c}$ (a.u.)
20	33	0.18[−1]	30	0.82[−3]	35	0.26[−3]
30	30	0.48[−2]	30	0.39[−3]	30	0.12[−3]
40	28	0.14[−2]	28	0.13[−3]	28	0.60[−4]
50	27	0.32[−3]	27	0.58[−4]	26	0.38[−4]
60	26	0.59[−4]	26	0.24[−4]	25	0.12[−4]
70	25	0.96[−4]	25	0.10[−5]	24	0.80[−5]
80	25	0.45[−4]	24	0.25[−4]	24	0.10[−4]
90	24	0.65[−4]	24	0.10[−5]	23	0.10[−5]
100	24	0.12[−4]	24	0.10[−5]	23	0.20[−5]
110	24	0.35[−4]	23	0.90[−5]	23	0.30[−5]
120	23	0.62[−4]	23	0.30[−5]	22	0.20[−5]
130	23	0.23[−4]	23	0.20[−5]	22	0.10[−5]
140	23	0.17[−4]	23	0.20[−5]	22	0.10[−5]
150	23	0.14[−4]	23	0.30[−5]	22	0.10[−6]
160	23	0.14[−4]	23	0.30[−5]	22	0.10[−6]
170	23	0.14[−4]	23	0.30[−5]	22	0.10[−6]
180	23	0.14[−4]	23	0.30[−5]	22	0.10[−6]
190	23	0.13[−4]	22	0.20[−5]	22	0.10[−6]
200	23	0.13[−4]	22	0.20[−5]	22	0.10[−6]

elastic cross sections for $1s$-$2s$ excitation of hydrogen atom by positron impact at the energies 54.5 eV, 100 eV, 200 eV, and 300 eV are given in Table III along with the predictions of Walters [32], Byron *et al.* [33], Bransden *et al.* [34], Mukherjee *et al.* [39], Morgan [35]. It follows that the present results are in good agreement with those predictions. We have further compared our present results for total cross sections with the 33-state approximation of Kernoghan *et al.* [41] in Fig. 3. It follows that the present results are in good agreement with all those predictions. It is important to note that though there exist differences in the differential cross sections near the forward scattering angle for different approximations the total cross sections predicted by different approximations are nearly equal. This is due to the fact that the differential cross sections, when integrated over the solid angle to yield total cross sections, have negligible contribution at the very forward scattering angles owing to the multiplicative factor $\sin\theta$ in Eq. (29). The major contribution to the total cross section comes from the differential cross sections at the intermediate scattering angles.

B. Positronium formation in positron-hydrogen collisions

Using the post form of the T-matrix of Eq. (7) we have

$$\begin{aligned} T_{fi}(\vec{k}_f,\vec{k}_i) &= \langle \chi_f^- | V_f - U_f | \chi_i^+ \rangle \\ &= \langle \chi_f^- | V_f | \chi_i^+ \rangle \\ &= \langle \Phi_f + G_f^- U_f \Phi_f | V_f | \Phi_i + G_i^+ U_i \Phi i \rangle \\ &= \langle \Phi_f | V_f | \Phi_i \rangle + \langle \Phi_f | V_f | G_i^+ U_i \Phi_i \rangle. \end{aligned} \tag{30}$$

In this case

$$U_i = \langle \phi_i | V_i | \phi_i \rangle = \langle \phi_{1s} | V_i | \phi_{1s} \rangle = \left(\frac{1}{r_1} + \lambda_i \right) e^{-\beta r_1},$$

$$U_f = \langle \phi_f | V_f | \phi_f \rangle = \langle \eta_f | V_f | \eta_f \rangle = 0,$$

where $V_i = (\frac{1}{r_1} - \frac{1}{r_{12}})$, $V_f = (\frac{1}{r_1} - \frac{1}{r_2})$, $\phi_i = \sqrt{\frac{\lambda_i^3}{\pi}} e^{-\lambda_i r_2}$, $\beta = 2\lambda_i, \lambda_i = 1$ with the plane wave states in the incident and the final channel given by

$$\Phi_i(\vec{r}_1, \vec{r}_2) = e^{i\vec{k}_i \cdot \vec{r}_1} \phi_i(\vec{r}_2) \quad \text{and } \Phi_f(\vec{r}_{12}, \vec{s}_{12}) = e^{i\vec{k}_f \cdot \vec{s}_{12}} \eta_f(\vec{r}_{12})$$

in atomic units. $s_{12} = (\vec{r}_1 + \vec{r}_2)/2$ being the coordinates of the center of mass of Ps atom and $\eta_f(\vec{r}_{12})$ are the wave function of Ps atom, where f corresponds to $(nlm), n = 1, 2, 3$.

Using the same technique as of the preceding section we obtain the partial-wave distorted amplitude as.

$$A_{fi}^{(L)}(k_f, k_i) = g_B^{(L)}(k_f, k_i) + D_{fi}^{(L)}(k_f, k_i), \tag{31}$$

1. Results and discussion:

We have computed the distorted-wave amplitudes (31) for each significant partial waves. Calculations for evaluating amplitudes for $(100) \to (n'00)$ transitions along with the method of evaluation of general three-denominator Lewis integral have been presented in the Appendixes. Our present partial-wave contributions to the ground state Ps formation cross section along with the corresponding summed up numbers giving total Ps$(1s)$ formation cross sections are presented in Table IV for some discrete energies in the range 20–300 eV. Table V exhibits the same event for $1s \rightarrow 2s$ and $1s \rightarrow 3s$ captures. From both Tables IV and V it is clear that the contribution to the total cross section, for all energies, as a function of partial wave is not monotonous. It is a clear indication, as we shall observe later, of the forward movement of critical angle.

Differential cross section and critical angle:Studies on the differential cross section for electron capture by an incoming positron reveal interesting findings. The differential cross section for Ps formation is obtained using the formula

$$\frac{d\sigma}{d\Omega} = 2\pi(v_f/v_i)\int_0^{\pi} |[A_{fi}(\vec{k}_f, \vec{k}_i)]|^2 \sin\theta_f \, d\theta_f \text{ (a.u.)}, \quad (32)$$

where $v_f = \hbar k_f/\mu_f, v_i = \hbar k_i/\mu_i, \theta_f = \hat{k}_i.\hat{k}_f$ is the scattering angle. We have approximated the higher partial-waves contribution to the distorted-wave amplitudes by the corresponding first Born amplitudes as the distorted-wave amplitudes reduce to the Born values for these partial waves so that the scattering amplitude is obtained as

$$[A_{fi}(\vec{k}_f, \vec{k}_i)] = \frac{1}{\sqrt{k_i k_f}} \sum_{l=0}^{L} (2l+1)[A_{fi}^{(l)}(k_f, k_i)]P_l(\cos\theta_f) + \frac{1}{\sqrt{k_i k_f}} \sum_{L+1}^{\infty} (2l+1) g_l^B(k_f, k_i) P_l(\cos\theta_f) \quad (33)$$

$$= \frac{1}{\sqrt{k_i k_f}} \sum_{l=0}^{L} (2l+1)([A_{fi}^{(l)}(k_f, k_i) - g_l^B(k_f, k_i)])P_l(\cos\theta_f) \quad (34)$$

$$+ g_B(\vec{k}_f, \vec{k}_i), \quad (35)$$

where the FBA amplitude

$$g_B(\vec{k}_f, \vec{k}_i) = (-\mu_f/2\pi)\Phi_f|V_f|\Phi_i \quad (36)$$

$$= \frac{1}{\sqrt{k_i k_f}} \sum_{l=0}^{\infty} (2l+1) g_l^B(k_f, k_i) P_l(\cos\theta_f), \quad (37)$$

$P_l(\cos\theta_f)$ denotes the Legendre polynomial of the first kind of order $l, \theta_f = \hat{k}_f.\hat{k}_i$ is the scattering angle, and L is the number of partial waves up to which the contribution of distorted-wave amplitudes have been taken into account.

The accuracy of the values of $d\sigma/d\Omega$ has been examined by integrating the differential cross sections over the entire solid angle to obtain the total cross appropriately produces low differential cross section as

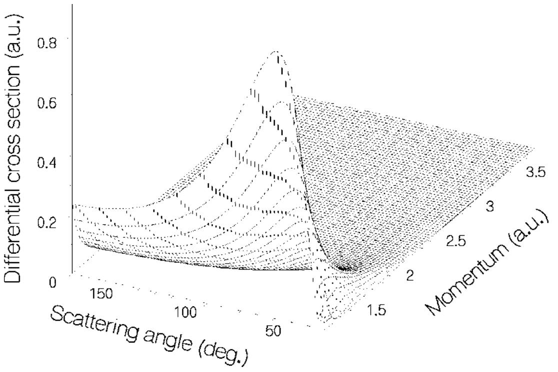

FIG. 6. Differential cross sections (a.u.) as a function of incident momentum (a.u.) and the scattering angle (30°–180°) for the reaction $e^+ + \mathrm{H}(1s) \rightarrow \mathrm{Ps}(1s) + \mathrm{H}^+$ in the energy range 20–200 eV.

$$\sigma = 2\int_{-1}^{1} \left(\frac{d\sigma}{d\Omega}\right) d(\cos\theta) \quad (\text{in units of } \pi a_0^2). \quad (38)$$

This formula (38) reproduces the same results for total cross sections as obtained by summing up the partial-wave contribution.

The differential cross section as a function of scattering angle and incident energy for all three capture processes have been calculated by using distorted-wave amplitudes. The tabulated values of differential cross sections at some of the scattering angles for the capture processes $1s \rightarrow 1s, 1s \rightarrow 2s$ and $1s \rightarrow 3s$ have been shown in Table VI for the energies 50 and 100 eV. Further in Table VII our present differential cross sections for ground state Ps formation have been compared with similar other available results such as, distorted wave calculation of Shakeshafts *et al.* [27], second-order distorted wave calculation of Mandal *et al.* [25] and all-order distorted wave approximation of Mandal and Guha [26]. Our results are a little bit lower than all these calculations. Some graphs have been presented in Figs. 4 and 5. Figure 4 clearly indicates the movement of critical angle in the differential cross sections of Ps formation in the forward direction.

The critical angles for the transitions $(100) \rightarrow (n'00), n' = 1, 2, 3$ have been listed in Table VIII in the energy range 20–200 eV. For all the three capture processes the nature of movement of the critical angle is very similar. At the incident energy of 20 eV it lies around 30° to 35° and then with increasing energy it approaches very slowly in the forward direction. It ultimately stops moving at an angle 22° thus forming a primary minimum in the differential cross section therein. The curved tunnel in the surface plots of Figs. 6–10 clearly demonstrate this fact. Further from Fig. 4 and the surface plots of Figs. 6–10 is noted that though the differential cross sections, for all three capture processes, peak at the forward scattering angle, there also exists secondary maximum just beside the minimum. This secondary maximum peaks around 50° and prominently emerges in the energy range 30–40 eV. The crests in the Fig. 4 showing the secondary maximum start becoming flat with the increasing energy. As we have earlier stated in Refs. [48–50] that possible interferences of scattered waves of different angular momen-

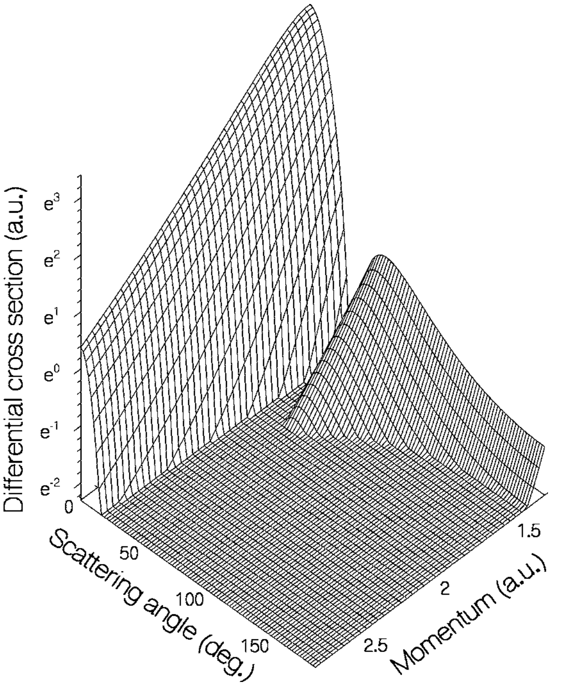

FIG. 7. Differential cross sections (a.u.) as a function of incident momentum (a.u.) and the scattering angle (0°–180°) for the reaction $e^+ + \mathrm{H}(1s) \rightarrow \mathrm{Ps}(1s) + \mathrm{H}^+$ in the energy range 20–100 eV.

tum states are responsible for such a nature of the differential cross section.

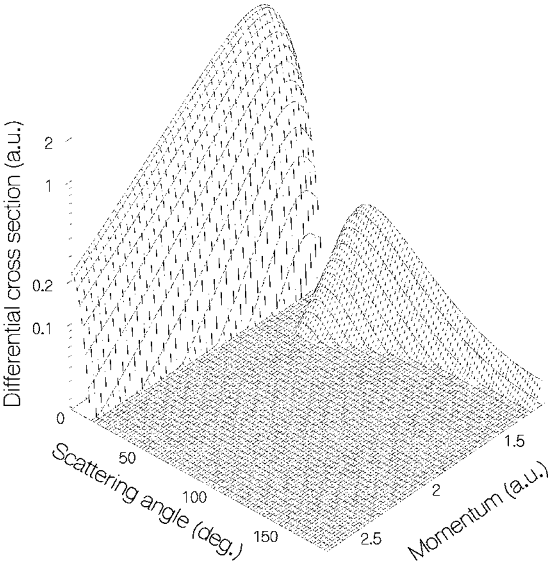

FIG. 9. Differential cross sections (a.u.) as a function of incident momentum (a.u.) and the scattering angle (0°–180°) for the reaction $e^+ + \mathrm{H}(1s) \rightarrow \mathrm{Ps}(2s) + \mathrm{H}^+$ in the energy range 20–100 eV.

Total cross section:We have presented our integrated cross section results for Ps formation along with the other distorted-wave results in Table IX. Our results for ground state Ps formation cross section are higher than distorted wave results of Shakeshafts *et al.* [27] but lower than the distorted-wave results of Mandal and Guha [26] Mandal and Guha, and Sil [25] except at the energy of 20 eV. It is interesting to note that the present distorted-wave results for ground state Ps formation cross section become coincident with our Schwinger's results [49] from the incident energy of 50 eV. We have compared our results for ground state Ps formation cross section with other theoretical and experimental predictions in Fig. 11. Though our results are nearly equal with experimental data of Weber *et al.* [45] at 20 eV and 30 eV, these are slightly lower than the 33-state approximation of Kernoghan *et al.* [41] and integral form of CCA of Basu *et al.* [44]. Beyond 30 eV the experimental results of Weber *et al.* [45] are higher than our prediction as well as the prediction of Kernoghan *et al.* [41]. It is clear from Fig. 11 that our results are close to those of Kernoghan *et al.* [41] beyond 30 eV.

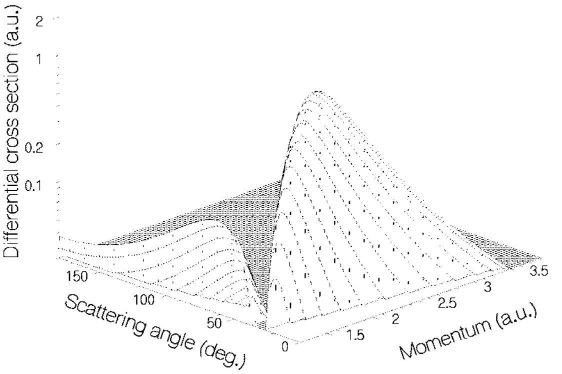

FIG. 8. Differential cross sections (a.u.) as a function of incident momentum (a.u.) and the scattering angle (0°–180°) for the reaction $e^+ + \mathrm{H}(1s) \rightarrow \mathrm{Ps}(2s) + \mathrm{H}^+$ in the energy range 20–200 eV.

The total cross section results of Ps formation in 2*s* state have been plotted in Fig. 12 along with the results of Kernoghan *et al.* [41]. Through the results of Kernoghan *et al.* [41] slightly increase first and then decrease with the increasing energy, our results steadily decrease for the lower energy

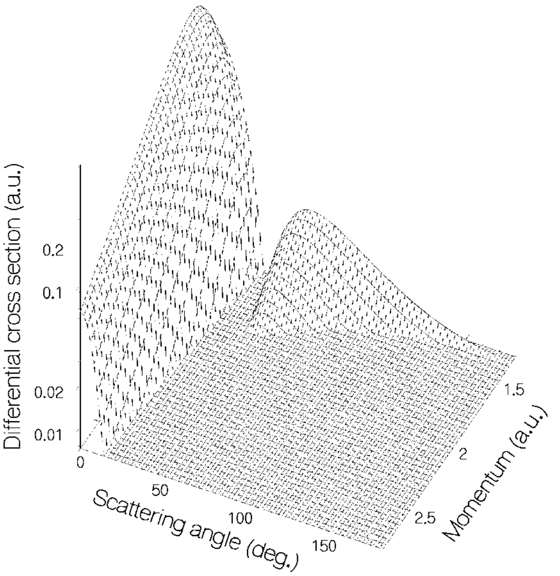

FIG. 10. Differential cross sections (a.u.) as a function of incident momentum (a.u.) and the scattering angle (0°–180°) for the reaction $e^+ + \mathrm{H}(1s) \rightarrow \mathrm{Ps}(2s) + \mathrm{H}^+$ in the energy range 20–100 eV.

TABLE IX. Integrated cross section, in units of πa_0^2, as a function of impact energy, for the reaction $e^+ + \mathrm{H}(1s) \rightarrow \mathrm{Ps}(n's) + p$. The notation $a[-b]$ means $a \times 10^{-b}$.

		Energy (eV)				
		20	50	100	200	300
$e^+ + \mathrm{H}(1s) \rightarrow \mathrm{Ps}(1s) + p$	DWA[a]	3.67	4.89[−1]	4.89[−2]	2.70[−3]	3.97[−4]
	SW[b]	2.2	4.3[−1]	4.8[−2]	3.0[−3]	
	MGS[c]	3.3	5.1[−1]	5.7[−2]	3.8[−3]	
	MG[d]	3.4	5.5[−1]	6.1[−1]	3.8[−3]	
	FBA	3.34	4.64[−1]	4.58[−2]	2.51[−3]	3.68[−4]
$e^+ + \mathrm{H}(1s) \rightarrow \mathrm{Ps}(2s) + p$	DWA[a]	3.62[−1]	6.87[−2]	7.29[−3]	3.93[−4]	5.64[−5]
	FBA	2.28[−1]	6.56[−2]	6.87[−3]	3.61[−4]	5.1[−5]
$e^+ + \mathrm{H}(1s) \rightarrow \mathrm{Ps}(3s) + p$	DWA[a]	6.79[−2]	2.04[−2]	2.18[−3]	1.19[−4]	1.8[−5]
	FBA	5.49[−2]	1.98[−2]	2.09[−3]	1.07[−4]	1.5[−5]

[a] Present calculation.
[b] Reference [27].
[c] Reference [25].
[d] Reference [26].

and then for the higher energy these decrease very slowly to become almost flat. Beyond 60 eV of incident energy our results become coincident with those of Kernoghan *et al.* [41].

It is clear from the graph plotted by Hewitt *et al.* [46] that the curves of total cross Ps formation in $2s$ state differ significantly for different approximations below the impact energy 60 eV. The authors considered (close-coupled approximation) CCA for two basis sets, UBA (unitary Born approximation) for two basis sets, and distorted curves by Khan *et al.* [47]. Even the 18-state approximation curve of Kernoghan *et al.* [42] has some fluctuation below 50 eV and significantly differs from the 33-state approximation curve of Kernoghan *et al.* [41].

IV. CONCLUSIONS

The scattering amplitude in the framework of distorted-wave formalism has conveniently been derived by approximating the distortion potential in a particular channel as the average of perturbation of that particular channel over the bound states. The present form of the theory allows one to calculate the scattering amplitude for all partial waves. The most advantage of this method is that a few straightforward calculations are required to compute the scattering amplitude. We have successfully applied this method to $1s$-$2s$ excitation of hydrogen atom by positron impact and positronium formation in positron-hydrogen collisions. The inability of the present method to account for the loss of inelastic flux appropriately produces low differential cross section for inelastic scattering near the very forward scattering angle, though there exists discrepancies regarding this in different theoretical investigations. Yet the total inelastic cross sections predicted by this theory are in good agreement with the other approximations. For rearrangement collisions this method works well in the intermediate and high energy range. So it seems plausible that the method may conveniently be applied to heavy projectiles also.

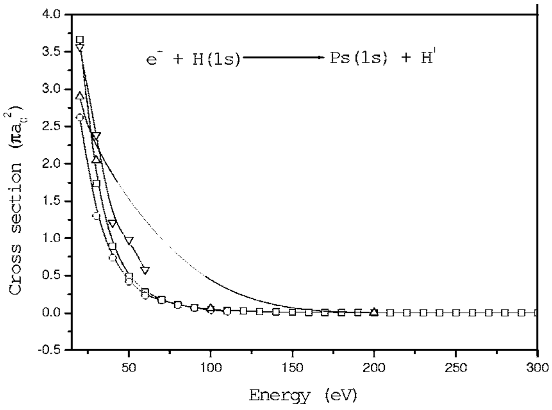

FIG. 11. Total positronium formation cross section (in units of πa_0^2) in ground state in positron-hydrogen collisions in the energy range 20–300 eV. Open square, present result; open circle, Kernoghan *et al.* [41]; triangle, Basu *et al.* [44]; inverted triangle, Weber *et al.* experiment [45].

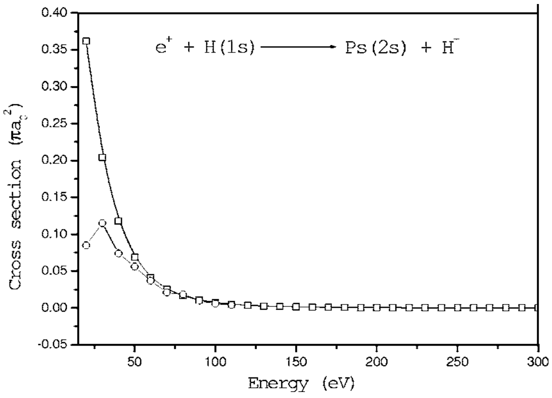

FIG. 12. Total positronium formation cross section (in units of πa_0^2) in $2s$ state in positron-hydrogen collisions in the energy range 20–300 eV. Open square, present result; open circle, Kernoghan *et al.* [41].

ACKNOWLEDGMENTS

One of the authors (A.G.) wishes to thank University Grants Commission (UGC), New Delhi for financial support through a Minor Research Project [Grant No. F. PSW-006/03-04 (ERO)].

APPENDIXA A: EVALUATION OF A GRNERAL THREE-DENOMINATOR LEWIS INTEGRAL

The three-denominator Dalitz integral

$$\frac{1}{\pi^2}\int \frac{d\vec{p}}{(p^2-k^2-i\epsilon)(|\vec{p}-\vec{v}_1|^2+\lambda_1^2)(|\vec{p}-\vec{v}_2|^2+\lambda_2^2)} \tag{A1}$$

appears in the second-Born amplitude and was first evaluated in a closed form by Dalitz [51]. Later Lewis [52] encountered the same integral while studying electron scattering by potentials using the second-Born approximation and considered a more general representation:

$$\begin{aligned}L_{111}(\delta;\vec{v}_1,\lambda_1;\vec{v}_2,\lambda_2) &= \frac{1}{\pi^2}\int \frac{d\vec{p}}{(p^2+\delta^2)(|\vec{p}-\vec{v}_1|^2+\lambda_1^2)(|\vec{p}-\vec{v}_2|^2+\lambda_2^2)}\\ &= \frac{1}{N^{\frac{1}{2}}}\ln\frac{\beta+N^{\frac{1}{2}}}{\beta-N^{\frac{1}{2}}},\end{aligned} \tag{A2}$$

where

$$N=\beta^2-\alpha\gamma, \tag{A3}$$

$$\begin{aligned}\beta &= \delta\left[|\vec{v}_1-\vec{v}_2|^2+(\lambda_1+\lambda_2)^2\right]+\lambda_1\left(v_2^2+\lambda_2^2+\delta^2\right)\\ &\quad+\lambda_2\left(v_1^2+\delta^2+\lambda_1^2\right),\end{aligned} \tag{A4}$$

$$\alpha\gamma=\left[|\vec{v}_1-\vec{v}_2|^2+(\lambda_1+\lambda_2)^2\right]\left[v_1^2+(\delta+\lambda_1)^2\right]\left[v_2^2+(\delta+\lambda_2)^2\right]. \tag{A5}$$

The same integral appears in a variety of first-and higher-order approximations in electron-atom, positron-atom, ion-atom, and photon-atom collisions for elastic scattering, impact excitations, rearrangement and ionizing collisions [25,26,53–55]. Historically Gavrila [55] also studied the integral (A1) while working out the second Born amplitude for photon-atom collisions and arrived at the same result (A2) as that of Lewis [52]. He used an integral representation of the Coulomb Green's function in the momentum space. It was however proved by Sil and co-workers [53] that $\alpha\gamma-\beta^2$ is positive definite and $N^{\frac{1}{2}}=i\sqrt{\alpha\gamma-\beta^2}$. Thus the parent integral (A2) can be expressed analytically as (Roy *et al.* [53])

$$\begin{aligned}L_{111} &= \frac{1}{i\sqrt{\alpha\gamma-\beta^2}}\ln\frac{\beta+i\sqrt{\alpha\gamma-\beta^2}}{\beta-i\sqrt{\alpha\gamma-\beta^2}}\\ &= \frac{1}{i\sqrt{\alpha\gamma-\beta^2}}\ln\frac{Re^{i\Theta}}{Re^{-i\Theta}}=\frac{1}{i\sqrt{\alpha\gamma-\beta^2}}2i\Theta=\frac{2\Theta}{\sqrt{\alpha\gamma-\beta^2}},\end{aligned} \tag{A6}$$

where

$$R^2=\beta^2+\alpha\gamma-\beta^2=\alpha\gamma, \tag{A7}$$

$$\Theta=\arctan\left(\frac{\sqrt{\alpha\gamma-\beta^2}}{\beta}\right). \tag{A8}$$

The higher-order derivatives are supposedly obtained simply by differentiating (A6) with respect to $\delta,\lambda_1,\lambda_2$ so that higher powers in the denominator are generated [53,54]. In what follows we prescribe a viable method of evaluation of the most general three-denominator integral.

Method of evaluation:In this paper, we present a simple method to obtain the general integral

$$\begin{aligned}&L_{lmn}(\delta;\vec{v}_1,\lambda_1;\vec{v}_2,\lambda_2)\\ &\quad=\frac{1}{\pi^2}\int\frac{d\vec{p}}{(p^2+\delta^2)^l(|\vec{p}-\vec{v}_1|^2+\lambda_1^2)^m(|\vec{p}-\vec{v}_2|^2+\lambda_2^2)^n}.\end{aligned} \tag{A9}$$

These integrals are of utmost importance in variational and other higher-order calculations involving one-and two-electron systems in electron-atom, positron-atom, ion-atom, photon-atom scattering, and transitions to higher Rydberg states.

Writing $a=|\vec{p}-\vec{v}_1|^2+\lambda_1^2$, $b=|\vec{p}-\vec{v}_2|^2+\lambda_2^2$, we use the Feynman parametrization technique [56] to obtain

$$\frac{1}{a^m b^n}=\frac{(m+n-1)!}{(m-1)!\,(n-1)!}\int_0^1\frac{t^{m-1}(1-t)^{n-1}}{(|\vec{p}-\vec{\Lambda}|^2+\mu^2)^{m+n}}dt, \tag{A10}$$

where

$$\vec{\Lambda}=t\vec{v}_1+(1-t)\vec{v}_2, \tag{A11}$$

$$\mu^2=t\lambda_1^2+(1-t)\lambda_2^2+t(1-t)|\vec{v}_1-\vec{v}_2|^2. \tag{A12}$$

After interchanging the order of integration, we have

$$L_{lmn}=\frac{(m+n-1)!}{(m-1)!\,(n-1)!}\int_0^1 t^{m-1}(1-t)^{n-1}dtI_{lmn}, \tag{A13}$$

where

$$I_{lmn}=\frac{1}{\pi^2}\int\frac{d\vec{p}}{(p^2+\delta^2)^l(|\vec{p}-\vec{\Lambda}|^2+\mu^2)^{m+n}}. \tag{A14}$$

Choosing the vector $\vec{\Lambda}$ along the z axis of $\vec{p}=(p_x,p_y,p_z)=(p,\theta,\phi)$ such that $|\vec{p}-\vec{\Lambda}|^2=p^2+\Lambda^2-2p\Lambda\cos\theta=A-B\cos\theta$, with $A=p^2+\Lambda^2$ and $B=2p\Lambda$, this gives

$$I_{lmn}=\frac{1}{\pi^2}\int_0^\infty\int_0^\pi\int_0^{2\pi}\frac{p^2\sin\theta\,dpd\theta d\phi}{(p^2+\delta^2)^l(A-B\cos\theta)^{m+n}}. \tag{A15}$$

Performing integrations over the angular variables θ,ϕ, we obtain

$$I_{lmn} = \frac{2}{\pi}\int_0^\infty \frac{p^2dp}{(p^2+\delta^2)^l}\left(\frac{(A-Bt)^{-(m+n)+1}}{B[(m+n)-1]}\right)_{t=-1}^{t=1}$$
$$= \frac{2}{\pi(m+n-1)}\int_0^\infty \frac{p^2dp}{(p^2+\delta^2)^l}\frac{1}{B}\left(\frac{1}{(A-B)^{m+n-1}} - \frac{1}{(A+B)^{m+n-1}}\right)$$
$$= \frac{2}{\pi(m+n-1)}\int_0^\infty \frac{p^2dp}{(p^2+\delta^2)^l}\frac{(A+B)^{m+n-1}-(A-B)^{m+n-1}}{B(A^2-B^2)^{m+n-1}}.$$

Thus

$$L_{lmn} = \frac{2(m+n)!}{\pi(m-1)!\,(n-1)!}\int_0^1 t^{m-1}(1-t)^{n-1}dt \times\int_0^\infty \frac{p^2dp}{(p^2+\delta^2)^l}\frac{(A+B)^{m+n-1}-(A-B)^{m+n-1}}{B(A^2-B^2)^{m+n-1}}. \tag{A16}$$

This is our final result which is to be evaluated numerically. The double integrals over $[0,\,1]$ and $[0,\infty]$ are highly convergent for $\delta\neq 0, \forall\ l,m,n\in\mathbf{N}$. However for $\delta=0$ and $l\rangle 1$, the integrals L_{lmn} are divergent; these remain convergent whenever $l=1$ and $\forall\ m,n\in\mathbf{N}$.

We used transformations

$$t=\tfrac{1}{2}(1+y),\quad t\in[0,1], y\in[-1,1], \tag{A17}$$

$$p=c\frac{1+z}{1-z},\quad p\in[0,\infty), z\in[-1,1] \tag{A18}$$

to carry out the integrations numerically employing Gauss-Legendre quadrature. Only 16 points for the t-integration and 20 points for the p integration were found sufficient for convergent results in our test cases. One can use such values of c as would ensure prompt convergence in the radial integration. (Take $c=2.0$ for instance.)

APPENDIX B: APPLICATION TO 100→n'00 CAPTURE AMPLITUDES

The amplitudes for $100\rightarrow n'00$ capture process in $e^+ + \mathrm{H}(100)\rightarrow \mathrm{Ps}(n'00)+\mathrm{H}^+, n'=1,\,2,\,3$ are obtained by inserting the appropriate bound-states $\phi_{1s}(\vec{r}_2)$ for H($1s$) and $\eta_{1s}(\vec{r}_{12}), \eta_{2s}(\vec{r}_{12}), \eta_{3s}(\vec{r}_{12})$ for Ps($n's$). Evaluation of each of the transition amplitudes is implemented with the help of the Lewis integrals L_{lmn}. We show below the Ps formation amplitudes in FBA for transitions $1s\rightarrow n's$ in terms of these integrals. These amplitudes have been used in the calculation of matrix elements of the distorted-wave approximation (DWA) in Sec. III B 1.

1. Amplitude for 1*s*-1*s* transition

Taking Fourier integral transforms for functions of the form $\exp(-\lambda r)/r$, $\exp(-\lambda r)$,

$$\exp(-\lambda r)/r = \frac{1}{2\pi^2}\int \frac{e^{i\vec{p}\cdot\vec{r}}}{p^2+\lambda^2}d\vec{p}, \tag{B1}$$

$$\exp(-\lambda r) = \frac{\lambda}{\pi^2}\int \frac{e^{i\vec{p}\cdot\vec{r}}}{(p^2+\lambda^2)^2}d\vec{p}, \tag{B2}$$

and then utilizing the δ-function properties, such as,

$$\int e^{i(\vec{q}-\vec{\Delta})\cdot\vec{r}}f(\vec{q})d\vec{q}\,d\vec{r} = (2\pi)^3\int \delta(\vec{q}-\vec{\Delta})f(\vec{q})d\vec{q} = (2\pi)^3 f(\vec{\Delta}), \tag{B3}$$

we obtain

$$\int e^{i\vec{A}\cdot\vec{r}_1+i\cdot\vec{B}\cdot\vec{r}_2-ar_2-br_{12}}\frac{1}{r_2}d\vec{r}_1d\vec{r}_2 = 32\pi^2 b\frac{1}{(\Delta_1^2+a^2)(\Delta_2^2+b^2)^2}, \tag{B4}$$

$$\int e^{i\vec{A}\cdot\vec{r}_1+i\cdot\vec{B}\cdot\vec{r}_2-ar_2-br_{12}}\frac{1}{r_{12}}d\vec{r}_1d\vec{r}_2 = 32\pi^2 a\frac{1}{(\Delta_1^2+a^2)^2(\Delta_2^2+b^2)}, \tag{B5}$$

and

$$\int e^{i\vec{A}\cdot\vec{r}_1+i\cdot\vec{B}\cdot\vec{r}_2-ar_2-br_{12}}\frac{1}{r_1}d\vec{r}_1d\vec{r}_2$$
$$= 32ab\int \frac{d\vec{p}}{p^2(|\vec{p}+\vec{A}+\vec{B}|^2+a^2)^2(|\vec{p}+\vec{A}|^2+b^2)^2}$$
$$= 32\pi^2 abL_{122}(0;\vec{\Delta}_1,a;\vec{\Delta}_2,b), \tag{B6}$$

where $\vec{\Delta}_1=\vec{A}+\vec{B}$ and $\vec{\Delta}_2=\vec{A}$. Therefore

$$F_{11}^{(t)}(a,b,\vec{\Delta}_1,\vec{\Delta}_2) = \int e^{i\vec{A}\cdot\vec{r}_1+i\cdot\vec{B}\cdot\vec{r}_2-ar_2-br_{12}}\left(\frac{1}{r_1}-\frac{1}{r_2}\right)d\vec{r}_1d\vec{r}_2$$
$$= 32\pi^2\left(abL_{122}(0;\vec{\Delta}_1,a;\vec{\Delta}_2,b) - \frac{b}{(\Delta_1^2+a^2)(\Delta_2^2+b^2)^2}\right) \tag{B7}$$

and

$$F_{11}^{(r)}(a,b,\vec{\Delta}_1,\vec{\Delta}_2) = \int e^{i\vec{A}\cdot\vec{r}_1+i\cdot\vec{B}\cdot\vec{r}_2-ar_2-br_{12}}\left(\frac{1}{r_1}-\frac{1}{r_{12}}\right)d\vec{r}_1d\vec{r}_2$$
$$= 32\pi^2\left(abL_{122}(0;\vec{\Delta}_1,a;\vec{\Delta}_2,b) - \frac{a}{(\Delta_1^2+a^2)^2(\Delta_2^2+b^2)}\right). \tag{B8}$$

Differentiating Eqs. (B7) and (B8) with respect to a we get

$$F^{(t)}_{21}(a,b,\vec{\Delta}_1,\vec{\Delta}_2)=\int r_2 e^{i\vec{A}\cdot\vec{r}_1+i\cdot\vec{B}\cdot\vec{r}_2-ar_2-br_{12}}\left(\frac{1}{r_1}-\frac{1}{r_2}\right)d\vec{r}_1d\vec{r}_2$$
$$=-32\pi^2\Bigg(bL_{122}(0;\vec{\Delta}_1,a;\vec{\Delta}_2,b)-4a^2bL_{132}(0;\vec{\Delta}_1,a;\vec{\Delta}_2,b)-\frac{2ab}{(\Delta_1^2+a^2)^2(\Delta_2^2+b^2)^2}\Bigg)\qquad\text{(B9)}$$

and

$$F^{(r)}_{21}(a,b,\vec{\Delta}_1,\vec{\Delta}_2)=\int r_2 e^{i\vec{A}\cdot\vec{r}_1+i\cdot\vec{B}\cdot\vec{r}_2-ar_2-br_{12}}\left(\frac{1}{r_1}-\frac{1}{r_{12}}\right)d\vec{r}_1d\vec{r}_2$$
$$=-32\pi^2\Bigg(bL_{122}(0;\vec{\Delta}_1,a;\vec{\Delta}_2,b)-4a^2bL_{132}(0;\vec{\Delta}_1,a;\vec{\Delta}_2,b)-\frac{1}{(\Delta_1^2+a^2)^2(\Delta_2^2+b^2)}+\frac{4a^2}{(\Delta_1^2+a^2)^3(\Delta_2^2+b^2)}\Bigg).\qquad\text{(B10)}$$

Further differentiation of Eqs. (B9) and (B10) with respect to a yields

$$F^{(t)}_{31}(a,b,\vec{\Delta}_1,\vec{\Delta}_2)=\int r_2^2 e^{i\vec{A}\cdot\vec{r}_1+i\cdot\vec{B}\cdot\vec{r}_2-ar_2-br_{12}}\left(\frac{1}{r_1}-\frac{1}{r_2}\right)d\vec{r}_1d\vec{r}_2$$
$$=32\pi^2\Bigg(-12abL_{132}(0;\vec{\Delta}_1,a;\vec{\Delta}_2,b)+24a^3bL_{142}(0;\vec{\Delta}_1,a;\vec{\Delta}_2,b)+\frac{2b}{(\Delta_1^2+a^2)^2(\Delta_2^2+b^2)^2}-\frac{8a^2b}{(\Delta_1^2+a^2)^3(\Delta_2^2+b^2)^2}\Bigg)\qquad\text{(B11)}$$

and

$$F^{(r)}_{31}(a,b,\vec{\Delta}_1,\vec{\Delta}_2)=\int r_2^2 e^{i\vec{A}\cdot\vec{r}_1+i\cdot\vec{B}\cdot\vec{r}_2-ar_2-br_{12}}\left(\frac{1}{r_1}-\frac{1}{r_{12}}\right)d\vec{r}_1d\vec{r}_2$$
$$=32\pi^2\Bigg(-12abL_{132}(0;\vec{\Delta}_1,a;\vec{\Delta}_2,b)+24a^3bL_{142}(0;\vec{\Delta}_1,a;\vec{\Delta}_2,b)+\frac{12a}{(\Delta_1^2+a^2)^3(\Delta_2^2+b^2)}-\frac{24a^3}{(\Delta_1^2+a^2)^4(\Delta_2^2+b^2)}\Bigg).\qquad\text{(B12)}$$

It is however easy to verify the following integrals:

$$\int r_{12} e^{i\vec{A}\cdot\vec{r}_1+i\cdot\vec{B}\cdot\vec{r}_2-ar_2-br_{12}}\left(\frac{1}{r_1}-\frac{1}{r_2}\right)d\vec{r}_1d\vec{r}_2=F^{(r)}_{21}(b,a,\vec{\Delta}_2,\vec{\Delta}_1),\qquad\text{(B13)}$$

$$\int r_{12} e^{i\vec{A}\cdot\vec{r}_1+i\cdot\vec{B}\cdot\vec{r}_2-ar_2-br_{12}}\left(\frac{1}{r_1}-\frac{1}{r_{12}}\right)d\vec{r}_1d\vec{r}_2=F^{(t)}_{21}(b,a,\vec{\Delta}_2,\vec{\Delta}_1),\qquad\text{(B14)}$$

$$\int r_{12}^2 e^{i\vec{A}\cdot\vec{r}_1+i\cdot\vec{B}\cdot\vec{r}_2-ar_2-br_{12}}\left(\frac{1}{r_1}-\frac{1}{r_2}\right)d\vec{r}_1d\vec{r}_2=F^{(r)}_{31}(b,a,\vec{\Delta}_2,\vec{\Delta}_1),\qquad\text{(B15)}$$

$$\int r_{12}^2 e^{i\vec{A}\cdot\vec{r}_1+i\cdot\vec{B}\cdot\vec{r}_2-ar_2-br_{12}}\left(\frac{1}{r_1}-\frac{1}{r_{12}}\right)d\vec{r}_1d\vec{r}_2=F^{(t)}_{31}(b,a,\vec{\Delta}_2,\vec{\Delta}_1).\qquad\text{(B16)}$$

We now calculate the $1s$-$1s$ transition amplitude $g_{1s,1s}$ in FBA as

$$g_{1s,1s}=\left(-\frac{\mu_f}{2\pi}\right)\langle\Phi_f|V_f|\Phi_i\rangle$$
$$=\left(-\frac{\mu_f}{2\pi}\right)\int\Phi_f^*V_f\Phi_i d\vec{r}_1d\vec{r}_2$$
$$=\left(-\frac{\mu_f}{2\pi}\right)\int e^{-i\cdot\vec{k}_f\cdot\vec{s}_{12}}\eta_{1s}(\vec{r}_{12})\left(\frac{1}{r_1}-\frac{1}{r_2}\right)e^{i\cdot\vec{k}_i\cdot\vec{r}_1}\phi_{1s}(\vec{r}_2)d\vec{r}_1d\vec{r}_2$$
$$=\left(-\frac{\mu_f}{2\pi}\right)N_f^*N_i\int e^{i(\vec{k}_i-(\vec{k}_f/2)).\vec{r}_1+i(-\vec{k}_f/2).\vec{r}_2}\left(\frac{1}{r_1}-\frac{1}{r_2}\right)e^{-\lambda_ir_2-\lambda_fr_{12}}d\vec{r}_1d\vec{r}_2,\qquad\text{(B17)}$$

where

$$\Phi_i(\vec{r}_1,\vec{r}_2)=e^{i\vec{k}_i\cdot\vec{r}_1}\phi_{1s}(\vec{r}_2)$$

and

$$\Phi_f(\vec{r}_{12},\vec{s}_{12})=e^{i\vec{k}_f\cdot\vec{s}_{12}}\eta_{1s}(\vec{r}_{12}),$$

with $\phi_{1s}(\vec{r}_2)=N_ie^{-\lambda_i\cdot r_2}$, $\eta_{1s}(\vec{r}_{12})=N_fe^{-\lambda_f r_{12}}$, $N_i=\sqrt{\lambda_i^3/\pi}$, $N_f=\sqrt{\lambda_f^3/\pi}$, $\lambda_i=2\lambda_f=1/a_0=1$(a.u.). Therefore

$$g_{1s,1s}=CF^{(t)}_{11}(\lambda_i,\lambda_f,\vec{\Delta}_1,\vec{\Delta}_2),\qquad\text{(B18)}$$

where

$$C=\left(-\frac{\mu_f}{2\pi}\right)\sqrt{\frac{\lambda_i^3}{\pi}}\sqrt{\frac{\lambda_f^3}{\pi}}\quad\vec{\Delta}_1=\vec{k}_i-\vec{k}_f,\quad\vec{\Delta}_2=\frac{\vec{k}_f}{2}.\qquad\text{(B19)}$$

2. Amplitude for 1*s*-2*s* transition

The $1s$-$2s$ transition amplitude $g_{2s,1s}$ in FBA is given by

$$
\begin{aligned}
g_{2s,1s} &= \left(-\frac{\mu_f}{2\pi}\right)\langle\Phi_f|V_f|\Phi_i\rangle \\
&= \left(-\frac{\mu_f}{2\pi}\right)\int \Phi_f^* V_f \Phi_i d\vec{r}_1 d\vec{r}_2 \\
&= \left(-\frac{\mu_f}{2\pi}\right)\int e^{-i\cdot\vec{k}_f\cdot\vec{s}_{12}}\eta_{2s}(\vec{r}_{12}) \\
&\quad\times\left(\frac{1}{r_1}-\frac{1}{r_2}\right)e^{i\cdot\vec{k}_i\cdot\vec{r}_1}\phi_{1s}(\vec{r}_2)d\vec{r}_1 d\vec{r}_2 \\
&= \left(-\frac{\mu_f}{2\pi}\right)N_f^* N_i \int e^{i\left(\vec{k}_i-\frac{\vec{k}_f}{2}\right)\cdot\vec{r}_1+i\left(-\frac{\vec{k}_f}{2}\right)\cdot\vec{r}_2}(2-\lambda_f r_{12}) \\
&\quad\times\left(\frac{1}{r_1}-\frac{1}{r_2}\right)e^{-\lambda_i r_2-\frac{\lambda_f}{2}r_{12}}d\vec{r}_1 d\vec{r}_2,
\end{aligned} \tag{B20}
$$

where

$$\Phi_i(\vec{r}_1,\vec{r}_2) = e^{i\vec{k}_i\cdot\vec{r}_1}\phi_{1s}(\vec{r}_2)$$

and

$$\Phi_f(\vec{r}_{12},\vec{s}_{12}) = e^{i\vec{k}_f\cdot\vec{s}_{12}}\eta_{2s}(\vec{r}_{12})$$

with $\phi_{1s}(\vec{r}_2)=N_i e^{-\lambda_i r_2}$, $\eta_{2s}(\vec{r}_{12})=N_f(2-\lambda_f r_{12})e^{-(\lambda_f/2)}r_{12}$, $N_i=\sqrt{\lambda_i^3/\pi}$, $N_f=\sqrt{\lambda_f^3/32\pi}$, $\lambda_i=2\lambda_f=1/a_0=1$(a.u.). Therefore

$$g_{2s,1s} = \frac{1}{4\sqrt{2}}C\left[2F_{11}^{(t)}\left(\lambda_i,\frac{\lambda_f}{2},\vec{\Delta}_1,\vec{\Delta}_2\right)-\lambda_f F_{21}^{(r)}\left(\frac{\lambda_f}{2},\lambda_i,\vec{\Delta}_2,\vec{\Delta}_1\right)\right]. \tag{B21}$$

3. Amplitude for 1*s*-3*s* transition

Finally 1*s*-3*s* transition amplitude $g_{3s,1s}$ in FBA is of the form

$$
\begin{aligned}
g_{3s,1s} &= \left(-\frac{\mu_f}{2\pi}\right)\langle\Phi_f|V_f|\Phi_i\rangle \\
&= \left(-\frac{\mu_f}{2\pi}\right)\int \Phi_f^* V_f \Phi_i d\vec{r}_1 d\vec{r}_2 \\
&= \left(-\frac{\mu_f}{2\pi}\right)\int e^{-i\cdot\vec{k}_f\cdot\vec{s}_{12}}\eta_{3s}(\vec{r}_{12}) \\
&\quad\times\left(\frac{1}{r_1}-\frac{1}{r_2}\right)e^{i\cdot\vec{k}_i\cdot\vec{r}_1}\phi_{1s}(\vec{r}_2)d\vec{r}_1 d\vec{r}_2 \\
&= \left(-\frac{\mu_f}{2\pi}\right)N_f^* N_i \int e^{i[\vec{k}_i-(\vec{k}_f/2)]\cdot\vec{r}_1+i(-\vec{k}_f/2)\cdot\vec{r}_2}(27-18\lambda_f r_{12} \\
&\quad+2\lambda_f^2 r_{12}^2)\left(\frac{1}{r_1}-\frac{1}{r_2}\right)e^{-\lambda_i r_2-(\lambda_f/3)r_{12}d\vec{r}_1 d\vec{r}_2},
\end{aligned} \tag{B22}
$$

where

$$\Phi_i(\vec{r}_1,\vec{r}_2) = e^{i\vec{k}_i\cdot\vec{r}_1}\phi_{1s}(\vec{r}_2)$$

and

$$\Phi_f(\vec{r}_{12},\vec{s}_{12}) = e^{i\vec{k}_f\cdot\vec{s}_{12}}\eta_{3s}(\vec{r}_{12})$$

with $\phi_{1s}(\vec{r}_2)=N_i e^{-\lambda_i r_2}$, $\eta_{3s}(\vec{r}_{12})=N_f(27-18\lambda_f r_{12}+2\lambda_f^2 r_{12}^2)e^{-(\lambda_f/3)r_{12}}$, $N_i=\sqrt{\lambda_i^3/\pi}$, $N_f=\frac{1}{81}\sqrt{\lambda_f^3/3\pi}$, $\lambda_i=2\lambda_f=1/a_0=1$(a.u.). Therefore

$$
\begin{aligned}
g_{3s,1s} = C\frac{1}{81\sqrt{3}}\Bigg[&27F_{11}^{(t)}\left(\lambda_i,\frac{\lambda_f}{3},\vec{\Delta}_1,\vec{\Delta}_2\right)-18\lambda_f F_{21}^{(r)} \\
&\times\left(\frac{\lambda_f}{3},\lambda_i,\vec{\Delta}_2,\vec{\Delta}_1\right)+2\lambda_f^2 F_{31}^{(r)}\left(\frac{\lambda_f}{3},\lambda_i,\vec{\Delta}_2,\vec{\Delta}_1\right)\Bigg].
\end{aligned} \tag{B23}
$$

---

[1] G. A. Erskine and H. S. W. Massey, Proc. R. Soc. London, Ser. A **212**, 521 (1952).

[2] V. I. Ochkur, Vestn. Leningr. Univ., Ser. 4: Fiz., Khim. **4**, 53 (1958).

[3] H. S. W. Massey and B. L. Moiseiwitch, Proc. R. Soc. London, Ser. A **227**, 38 (1954).

[4] H. S. W. Massey and B. L. Moiseiwitch, Proc. R. Soc. London, Ser. A **258**, 147 (1960).

[5] R. Marriott, Proc. Phys. Soc., London, Sect. A **70**, 288 (1957).

[6] S. Khashaba and H. S. W. Massey, Proc. Phys. Soc. London **71**, 574 (1958).

[7] T. Swada, J. E. Purcell and A. E. Green, Phys. Rev. A **4**, 193 (1971).

[8] D. H. Madison and W. N. Shelton, Phys. Rev. A **7**, 499 (1973); **7**, 514 (1973).

[9] B. H. Bransden and M. R. C. McDowell, Phys. Lett., C **30C**, 207 (1977); **46**, 249 (1978).

[10] L. E. Machado, E. P. Leal, and G. Csanak, J. Phys. B **15**, 1773 (1982); Phys. Rev. A **29**, 1811 (1984).

[11] N. T. Padial, G. D. Meneses, F. J. da Paixao, G. Csanak, and D. C. Cartwright, Phys. Rev. A **23**, 2194 (1981).

[12] G. D. Meneses, L. E. Machado, G. Csanak, and D. C. Cartwright, J. Phys. B **20**, L717 (1987).

[13] D. H. Madison, Phys. Rev. Lett. **53**, 42 (1984).

[14] D. H. Madison, I. A. Hughes, and D. S. McGinnes, J. Phys. B **18**, 2737 (1985).

[15] D. H. Madison and K. H. Winters, J. Phys. B **20**, 4173 (1987).

[16] D. H. Madison, K. H. Winters, and S. L. Downing, J. Phys. B **22**, 1651 (1989).

[17] D. H. Madison, I. Bray, and I. E. McCarthy, J. Phys. B **24**, 3861 (1991).

[18] C. Zhangjin, D. H. Madison, T. W. Colm, and H. R. J. Walters, J. Phys. B **37**, 981 (2004).

[19] T. N. Rescigno, C. W. McCurdy, and V. Mckoy, J. Phys. B **7**, 2396 (1974); T. N. Rescigno, C. W. McCurdy, V. Mckoy, and C. F. Bender, Phys. Rev. A **13**, 216 (1976).

[20] A. W. Fliflet and V. Mckoy, Phys. Rev. A **21**, 1863 (1980).

[21] M. T. Lee, L. E. Machado, E. P. Leal, L. M. Brescansin, M. A. P. Lima, and F. B. C. Machado, J. Phys. B **23**, L233 (1990).

[22] Mu-Tao Lee, R. R. Lucchese, and V. McKoy, Phys. Rev. A **26**,

3240 (1982).
[23] J. A. Levenson, and M. K. Banerjee, Ann. Phys. (N.Y.) **2**, 471 (1957).
[24] R. H. Bassel and E. Gerjuoy, Phys. Rev. **117**, 749 (1960).
[25] P. Mandal, S. Guha, and N. C. Sil, J. Phys. B **12**, 2913 (1979).
[26] P. Mandal and S. Guha, J. Phys. B **12**, 1603 (1979).
[27] R. Shakeshaft and J. M. Wadehra, Phys. Rev. A **22**, 968 (1980).
[28] P. Khan and A. S. Ghosh, Phys. Rev. A **27**, 1904 (1983).
[29] R. Srivastava, A. K. Katiyarm, and I. Khurana, J. Phys. B **20**, 1853 (1987).
[30] V. E. Bubelev and D. Madison, J. Phys. B **25**, 3229 (1992).
[31] J. Colgan, D. M. Mitnik, and M. S. Pindzola, Phys. Rev. A **63**, 012712 (2000).
[32] H. R. J. Walters, J. Phys. B **21**, 1893 (1988).
[33] F. W. Byron, Jr., C. J. Joachain, and R. M. Potvlieege, J. Phys. B **14**, L609 (1981).
[34] B. H. Bransden, I. E. McCarthy, and A. T. Stelbovics, J. Phys. B **18**, 823 (1985).
[35] L. A. Morgan, J. Phys. B **15**, L25 (1982).
[36] M. Gell-Mann and M. L. Goldberger, Phys. Rev. **91**, 398 (1953).
[37] J. R. Oppenheimer, Phys. Rev. **31**, 349 (1928).
[38] See G. C. Wick, in Ref. [37]).
[39] M. Mukherjee, M. Basu, and A. S. Ghosh, J. Phys. B **23**, 757 (1990).
[40] C. J. Joachain and R. M. Potvliege, Phys. Rev. A **38**, 4337 (1988).
[41] A. A. Kernoghan, D. J. R. Robinson, M. T. McAlinden, and H. R. J. Walters, J. Phys. B **29**, 2089 (1996).
[42] A. A. Kernoghan, M. T. McAlinden, and H. R. J. Walters, J. Phys. B **28**, 1079 (1995).
[43] J. D. Jackson and H. Shiff, Phys. Rev. **89**, 359 (1953).
[44] D. Basu, G. Banerji, and A. S. Ghosh, Phys. Rev. A **13**, 1381 (1976).
[45] M. Weber, A. Hofmann, W. Raith, W. Sperber, F. Jacobsen, and K. G. Lynn, Hyperfine Interact. **89**, 221 (1994).
[46] R. N. Hewitt, C. J. Noble, and B. H. Bransden, J. Phys. B **23**, 4185 (1990).
[47] P. Khan, P. S. Mazumdar, and A. S. Ghosh, Phys. Rev. A **31**, 1405 (1985).
[48] U. Roy and P. Mandal, J. Phys. B **22**, L261 (1989); **23**, L55 (1990); Phys. Rev. A **48**, 233 (1993); **48**, 2952 (1993).
[49] S. Kar and P. Mandal, J. Phys. B **73** L253 (1998); **32**, 2297 (1999); Phys. Rev. A **59**, 1913 (1999); J. Phys. B **33**, L165 (2000); Phys. Rev. A **62**, 052514 (2000).
[50] A. Ghoshal and P. Mandal (unpublished).
[51] R. H. Dalitz, Proc. R. Soc. London, Ser. A **206**, 509 (1951).
[52] R. R. Lewis, Jr., Phys. Rev. **102**, 537 (1956).
[53] U. Roy, L. J. Dube, P. Mandal, and N. C. Sil, Comput. Phys. Commun. **92**, 227 (1996).
[54] U. Roy and N. C. Sil, J. Phys. B **30**, 3423 (1997).
[55] M. Gavrila, Phys. Rev. **163**, 147 (1967); Z. Phys. **293**, 269 (1970).
[56] R. P. Feynman, Phys. Rev. **76**, 769 (1949).